JOURNAL OF GEOPHYSICAL RESEARCH, VOL. 88, NO. B12, PAGES 10,449–10,477, DECEMBER 10, 1983

# Gravity Anomalies and Flexure of the Lithosphere at Mountain Ranges

G. D. KARNER[1] AND A. B. WATTS

*Lamont-Doherty Geological Observatory and Department of Geological Sciences, Columbia University*

The Bouguer gravity anomaly over the Himalayan, Alpine, and Appalachian mountains is characterized by a generally asymmetric gravity "low," which spans the mountains and associated foreland basins. The minimum of the gravity "low" is generally systematically displaced from the region of greatest topographic relief and shows no obvious relationship to surface geology. In addition, the Alps and Appalachians are associated with a generally symmetric gravity "high" that is unrelated to the topographic relief. Together the gravity low and high form a characteristic positive-negative anomaly "couple." The steep gravity gradient between the positive and negative couple correlates with the Insubric line and its equivalents in the Alps and the Brevard Zone in the southern Appalachians. This gravity anomaly couple is interpreted as evidence for flexure of the continental lithosphere by subsurface (buried) and surface (topographic) loading. The magnitude of the subsurface load is estimated from the integrated excess mass represented by the positive anomaly and the magnitude of the surface load from the topography. By combining these loads the flexure of the lithosphere and the associated Bouguer gravity anomaly are calculated for different assumed values of the elastic thickness $T_e$ of continental lithosphere. The best fitting value of $T_e$ for the Himalayas is 80–100 km, for the Alps 25–50 km, and for the Appalachians 80-130 km. The model calculations suggest that the main contribution to the gravity couple in the Alps and Appalachians arises not from surface loads such as thrust sheets and nappes but from subsurface loads. However, in the case of the Himalayas the topography appears to be a sufficient load to explain the observed asymmetric gravity low. When subsurface loads do exist therefore, we would not expect a close correlation between mountain topographic relief and depth to the M discontinuity as required by classical models of isostasy. Rather, the M discontinuity is expected to relate to the center of mass of all the loads acting on the lithosphere. The surface and subsurface loads, inferred from the gravity anomaly, play a major role in the development of mountains and foreland basins. The emplacement of large subsurface loads represents the primary event in the Alps and Appalachians, while in the Himalayas the emplacement of the surface load is the primary event. The emplacement of the subsurface load probably marks the initiation of foreland basin development. The regional characteristics of the basin are controlled by the primary load, while local variations are controlled by the secondary, thrust sheet loads. Subsequent movement of either load will produce migration of the basin depocenter. The origin of the subsurface load is not clear, but its association with the insubric line in the Alps and the Brevard Zone in the Appalachians suggests that it may be related to the "obduction" of crustal blocks/flakes onto the underlying plate during continental collision or possibly to the preloaded crustal structure of the underlying plate.

## INTRODUCTION

The gravity field over orogenic belts has long been a subject of considerable interest to geodesists, geologists, and geophysicists. The gravity field is a sensitive indicator of the degree and the manner in which surficial topographic features on the earth are compensated at depth. The earliest gravity studies showed that regions of high topographic relief, such as the Andes and Himalaya, are compensated at depth. *Airy* [1855] proposed a model in which the compensation took the form of a thickening of a crust of uniform density. *Pratt* [1855], on the other hand, proposed that the compensation took the form of lateral density changes in a crust and upper mantle of equal overall thickness. In both models the compensation occurred directly beneath the topography, taking the shape of a deep crustal "root" in the Airy model and an overall mass deficiency in the crust and upper mantle in the Pratt model.

It was subsequently shown that these isostatic models satisfactorily reduced closure errors in geodetic surveys in mountainous terrain in the United States, India, and northern Europe [*Hayford and Bowie*, 1912; *Heiskanen*, 1924]. Many questions were raised, however, concerning the applicability of these models to understanding the geological processes involved in mountain building [e.g., *Chamberlin*, 1931]. Of particular concern was the origin of the topographic relief itself. Geological field mapping revealed that many mountain ranges were cored by relatively low-density granitic-type rocks but were flanked by folded sediments. This suggested that both vertical and horizontal movements may play a significant role in mountain building [e.g., *Bowie*, 1927]. Unfortunately, the Airy and Pratt isostatic models only provide a static description of the final configuration of the crustal and mantle structure and therefore provide no information on the relative importance of horizontal and vertical movements.

During the late nineteenth and early twentieth centuries a vigorous effort was made in the United States and Europe to obtain continuous profiles of the gravity field over mountain ranges [e.g., *Putnam*, 1895; *Heiskanen*, 1924]. These profiles showed that mountain ranges were characterized by large-amplitude positive and negative gravity anomalies that could not easily be explained by the Airy or Pratt models. In the case of the Alps a positive-negative anomaly "couple" was mapped that was nearly continuous along the entire mountain range. These, and other observations, prompted *Chamberlin* [1931] to conclude that the geological processes involved in mountain building occurred largely independent of isostasy. He stated, for example, that isostasy was more likely to act in opposition to mountain building.

[1] Also at Bureau of Mineral Resources, Australia.



Paper number 3B1158.
0148-0227/83/003B-1158$05.00

The first detailed interpretations of the positive-negative anomaly couple were in terms of "static" models for the distribution of mass in mountain ranges [e.g., *Kaminski and Menzel*, 1968; *Diment*, 1968; *Tanner and Uffen*, 1960; *Tanner*, 1969; *Mueller and Talwani*, 1971; *Choudhury et al.*, 1971]. In these studies the positive anomalies were generally interpreted as due to high-density rocks within the crust, while the flanking negative anomalies were interpreted as due to overthickened crust. The mass sections obtained were useful since they located regions of mass excess and deficiencies in mountain ranges. However, they provided little information on the geological processes and therefore the mechanisms that actually occur during mountain building.

Following the development of plate tectonics during the late 1960's, the positive-negative anomaly couple over mountain ranges was qualitatively reinterpreted in terms of plate convergence, suturing, and collision. *Brooks* [1970*a*, *b*], for example, suggested that the anomaly couple might be due to the overthrusting of one lithosphere plate (which included a crust) over an underlying plate during mountain building. In the case of the Alps, *Brooks* [1970*a*] pointed out that the positive anomaly correlated in position with the Ivrea Zone and that it represented high-density, lower crustal and/or upper mantle rocks. A similar suggestion was later made for selected gravity anomaly profiles of major structural provinces within the Canadian shield [*Gibb and Thomas*, 1976], the Musgrave and Fraser ranges in Australia [*Fountain and Salisbury*, 1981], the Kasila Range in West Africa [*Fountain and Salisbury*, 1981], and the Pyrenean Range in France and Spain [*Daignieres et al.*, 1982].

However, it is still not clear from these studies what the role of isostasy is in mountain building and what model(s), if any, can explain the gravity anomaly over mountain ranges. Classically, isostasy has been concerned with the compensation of surficial topography on the earth's surface. Mountain building, however, results from the complex interaction of vertical and horizontal forces associated with plate convergence. As a consequence, there is a redistribution of mass, for example, the obduction of oceanic crust, the development of accretionary wedges, and the mobilization of thrust sheets and nappes, that is superimposed either on or within lithospheric plates. The imbalance caused by this redistribution of mass is restored according to the principles of isostasy.

During the past few years our knowledge of the isostatic response of the lithosphere to surficial loads such as river deltas, ice sheets, and oceanic islands and seamounts has progressed rapidly [e.g., *Watts*, 1978; *Caldwell and Turcotte*, 1979; *Sandwell and Schubert*, 1982; *Menard and McNutt*, 1982]. Studies of these features suggest that the lithosphere responds to long duration ($\gtrsim 10^5$ years) loads in a manner similar to an elastic plate overlying a weak fluid. Oceanic flexure studies have shown that the flexural rigidity of the lithosphere (and its equivalent elastic thickness $T_e$) is a function of the age and hence thermal structure of the lithosphere at the time it was loaded. There is a good overall fit of $T_e$ to the depth of the 300°–600°C oceanic isotherms based on the cooling plate model, suggesting that as the lithosphere increases with age and cools, it becomes more rigid in its response to loads [*Watts et al.*, 1980]. Recently, we have used this model to explain a number of tectonostratigraphic features of sedimentary basins in passive continental margins and the continental interiors [*Karner and Watts*, 1982; *Watts et al.*, 1982].

An outstanding problem, therefore, is the role of flexure in controlling mountain building. The mechanism of mountain building involves the local transfer of material onto the continental lithosphere, and so we would expect a flexural control in the development of mountain ranges and their associated foreland basins. *Warsi and Molnar* [1977] and *Turcotte and Schubert* [1982] considered that flexure may be important in controlling the development of foreland basins flanking the Himalaya and Appalachian mountain ranges. They attributed basin development to bending of the underlying basement by applied loads developed during continental suturing and collision. *Jordan* [1981], in reconstructing the thrust/nappe loads based on detailed geological field mapping, showed that the load of the fold/thrust belts in the U.S. Rockies was insufficient to explain the development of the Denver and Powder River basins. She used large sediment loads, presumably due to erosion of the thrust sheets, and the existence of an unknown driving force to explain fully in the development of these basins. Further, she concluded that an elastic plate model was an adequate approximation for the response of the continental basement to these loads. *Beaumont* [1981], by assuming that the load was caused by laterally migrating thrust sheets in the Canadian Rockies, predicted the stratigraphy of the Alberta Basin. However, in order to match the observed stratigraphy he used a viscoelastic (Maxwell) model for the long-term mechanical properties of the continental lithosphere. As demonstrated by *Watts et al.* [1982], an elastic model in which the rigidity is a function of the age of the lithosphere adequately explains the stratigraphy of basins in other intracratonic settings.

The main difficulty with these previous flexure studies, however, is that the gravity field, which is a function of both the load and the mechanical properties of the lithosphere, was not used as a constraint. The purpose of this paper therefore is to describe the gravity anomaly patterns over orogenic belts and then to use these patterns to evaluate the role of lithospheric flexure in mountain building. We have selected three mountain ranges for the study; Himalaya, Alps, and Appalachians, for which a sufficient spatial distribution of gravity and topography data is available. These data will be used to evaluate quantitatively the relationship between gravity and topography at mountain ranges. The objective of the study is to determine the relative role of surface and subsurface loading in mountain building and to use this information to understand better the long-term mechanical properties of continental lithosphere.

## GEOLOGICAL SETTING

### *Himalayas*

Figure 1 shows a simplified geological map of the Himalayan region which defines the main tectonic/stratigraphic units. The geological history of the Himalayas can most easily be discussed in terms of two main stages: The first stage involved convergence of the northward drifting Indian subcontinent with a proto-Tibetan landmass during the Late Cretaceous and Paleocene, culminating in a lower-middle Eocene collision [*Powell and Conaghan*, 1973]. The second stage involved the formation of a fundamental detachment surface during the late Eocene/Oligocence (the main boundary fault) along which the Indian continental lithosphere was underthrust from Miocene to Recent [*Seeber et al.*, 1981]. As a consequence of this collision, a peripheral molasse basin (Ganges Basin) was produced which resulted in the deposition of Neogene clastics

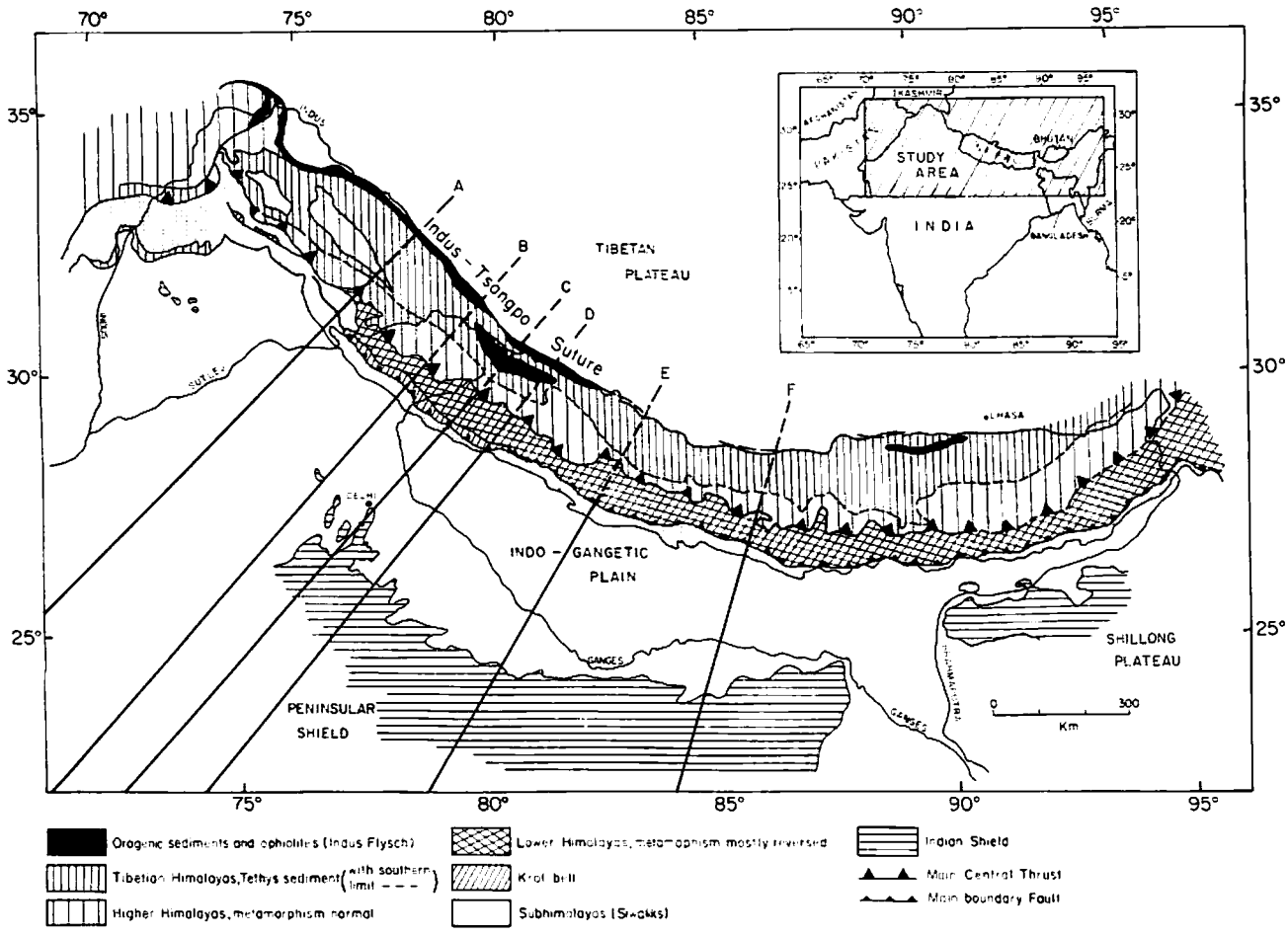


Fig. 1. Simplified geological map of northern India [*Gansser*, 1964], showing the main tectonic units of the foreland the Himalayan mountains. The heavy lines (A-F) represent the position of projected topographic and gravimetric data shown in Figure 4. These projection lines have been extended into Tibet only for ease of display. Data exist only where the projection line is solid.

onto older Paleozoic formations and Precambrian basement. Recent local reworking of the molasses sediments is occurring within the sub-Himalayas and near the Shillong Plateau. The Shillong Plateau (Figure 1) exists in a region of high seismicity generally parallel to the Himalayan trend. The large thrust-type earthquakes associated with this plateau suggest that it may be detached from the shield and overriding the Ganges Basin [*Chandra*, 1978].

The Ganges Basin (Figure 1) varies in width from 100 km in the east to 400 km in the west. The basin is asymmetric with a maximum depth of ~6 km at the base of the Siwaliks [*Sastri et al.*, 1971] and consists of upper Miocene to Recent molasse-type sediments which prograde onto the Indian shield with a general increase in grain size up-sequence [Powell and Conaghan, 1973].

The peninsular Indian shield (Figure 1) consists of metamorphic and crystalline rocks of Protozoic/Archacan age. Tholeiitic flood basalts (Deccan traps) of Late Cretaceous and Paleocene-Eocene age overlie shield rocks in the northwest. The Deccan traps were uplifted and eroded during Miocene times, contemporaneous with the main deformational phase in the Himalayas. This coeval development of the Ganges Basin and the uplift of the shield and Deccan traps led *Warsi and Molnar* [1977] to suggest that the uplifted portion of the Peninsula shield was analogous to the outer topographic rise observed by *Watts and Talwani* [1974] seaward of deep-sea trenches.

The Himalayan range can be subdivided ino two regions relative to the location of the Main Central Thrust (MCT) [*Seeber et al.*, 1981]. North of the MCT is the Tethyan Zone, which includes the High and Tethys Himalaya and the Tibetan Plateau. South of the MCT exists the sedimentary zone, which includes the complex nappes and thrust sheets of the Lesser Himalaya and both autochthonous and allochthonous units of the sub-Himalayas.

The Indus-Tsangpo suture (Figure 1), which is characterized by an ophiolitic complex, marks the first collisional contact between India and a continental or island arc terrain [*Powell*, 1979; *Klootwijk*, 1979]. The lack of present seismicity or topographic relief suggests that the suture is now tectonically inactive [*Seeber et al.*, 1981].

### *Alps*

The Alpine fold belt has had a long and complex history beginning with continental rifting and the development of passive continental margins in the Permo-Triassic, followed by thrusting and ophiolite obduction in the Cretaceous, culminating in a continent-continent collision with associated nappe and thrust sheet emplacement during the Oligocene-Miocene. Figure 2 summarizes the main geological features of

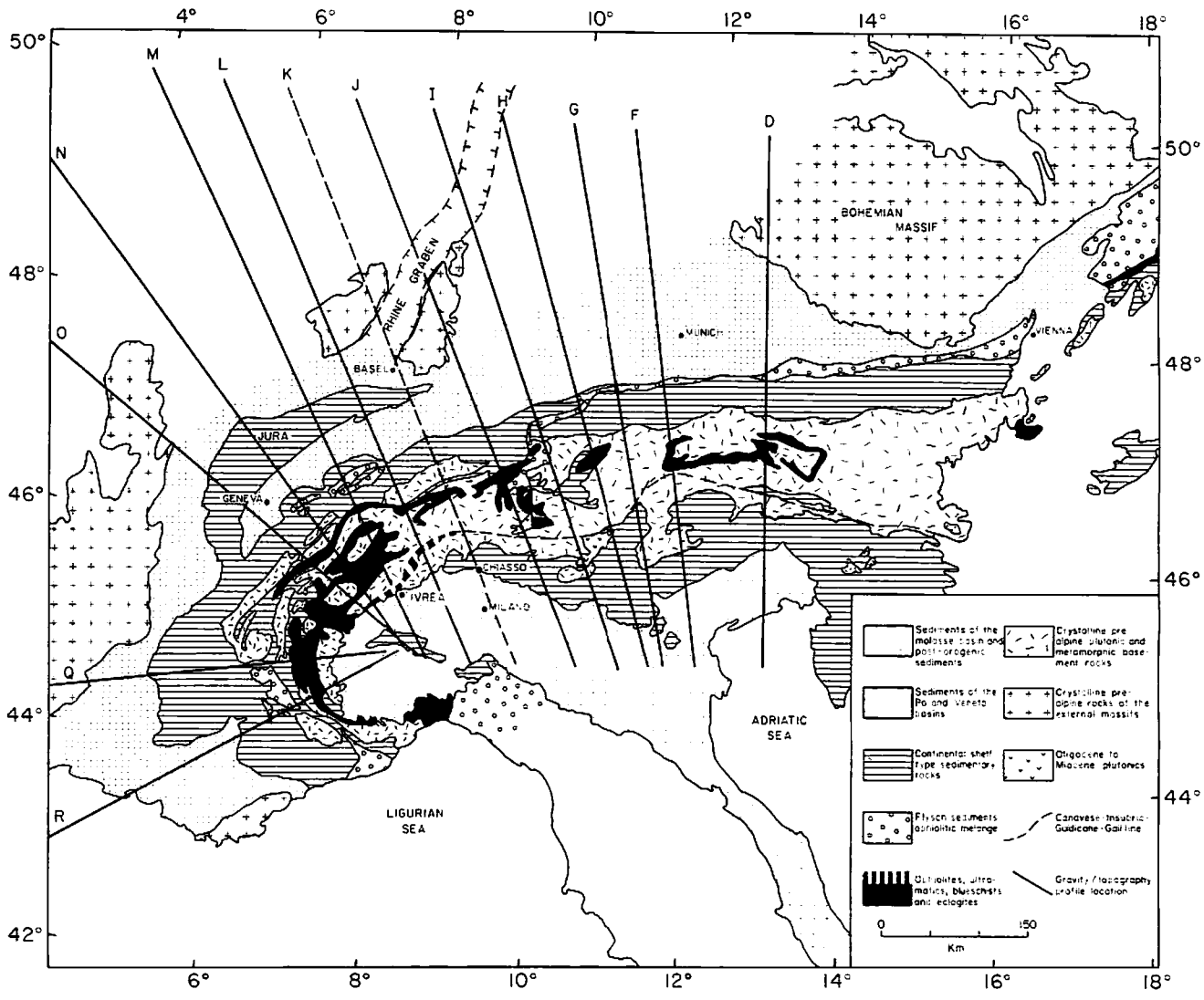


Fig. 2. Simplified geological map of the European Alpine system [*Dietrich*, 1979] showing the main tectonic units. The lines labeled D–R represent profiles of projected topographic and gravimetric data shown in Figure 5. In particular, profile K represents the position of the Swiss geotraverse [e.g., *Rybach et al.*, 1980].

the Alps. The geology can most conveniently be discussed by considering the rock units either side of the Insubric line, a lineament which separates geological units that have had very different development histories. The northern units are characterized by a stack of sedimentary and crystalline nappes (Penninic and Helvetic units), parts of which have undergone intense Alpine metamorphism. These nappes have been overthrust from the south onto Hercynian-aged basement of the European plate. In places, the basement has been actively involved in the thrusting and has given rise to partly detached crystalline massifs of the External Zone [*Laubsher*, 1973; *Hsü*, 1979; *Mueller et al.*, 1980; *Beach*, 1981]. The units south of the Insubric line, in contrast to the northern units, were not involved with any Alpine metamorphism.

In the area of Ivrea (Figure 2), ultrabasic rocks crop out along the Insubric line and represent upper mantle rocks exposed by large-scale overthrusting [e.g., *Lemoine*, 1978]. The Ivrea Zone has been interpreted as a crustal flake emplaced during the Hercynian orogeny and remobilized into the upper crust during the Alpine orogeny [*Schenk*, 1981].

The tectonic deformations which produced the nappes and large overthrusts in the Alps occurred in three principal phases: (1) the Cretaceous, especially the Late Cretaceous, (2) the late Eocene/early Oligocene, and (3) during the Neogene. In the western and central Alps at least, these three phases characterize the Austro-Alpine, Penninic, and Helvetic domains, respectively.

The Jura Mountains in France and Switzerland mainly consist of folded platform carbonates decoupled from the underlying Hercynian basement by a decollement surface in Triassic evaporites [*Müller and Briegel*, 1980]. The folding represents a maximum horizontal shortening of 30 km [*Laubscher*, 1981]. The principal folding event which ruptured the cover, producing overthrusts within the Jura, occurred in the late Miocene/early Pliocene.

The northern Alpine foredeep, the Molasse Basin, consists of continental and marine molassic deposits, mainly sandstones and conglomerates. They were deposited in an asymmetric basin with a maximum thickness of 3–5 km near the base of the Alps, where the sediments are reworked into folds and thrusts (the sub-Alpine molasse). Sediments within the basin onlap toward the foreland [e.g., *Clar*, 1973].

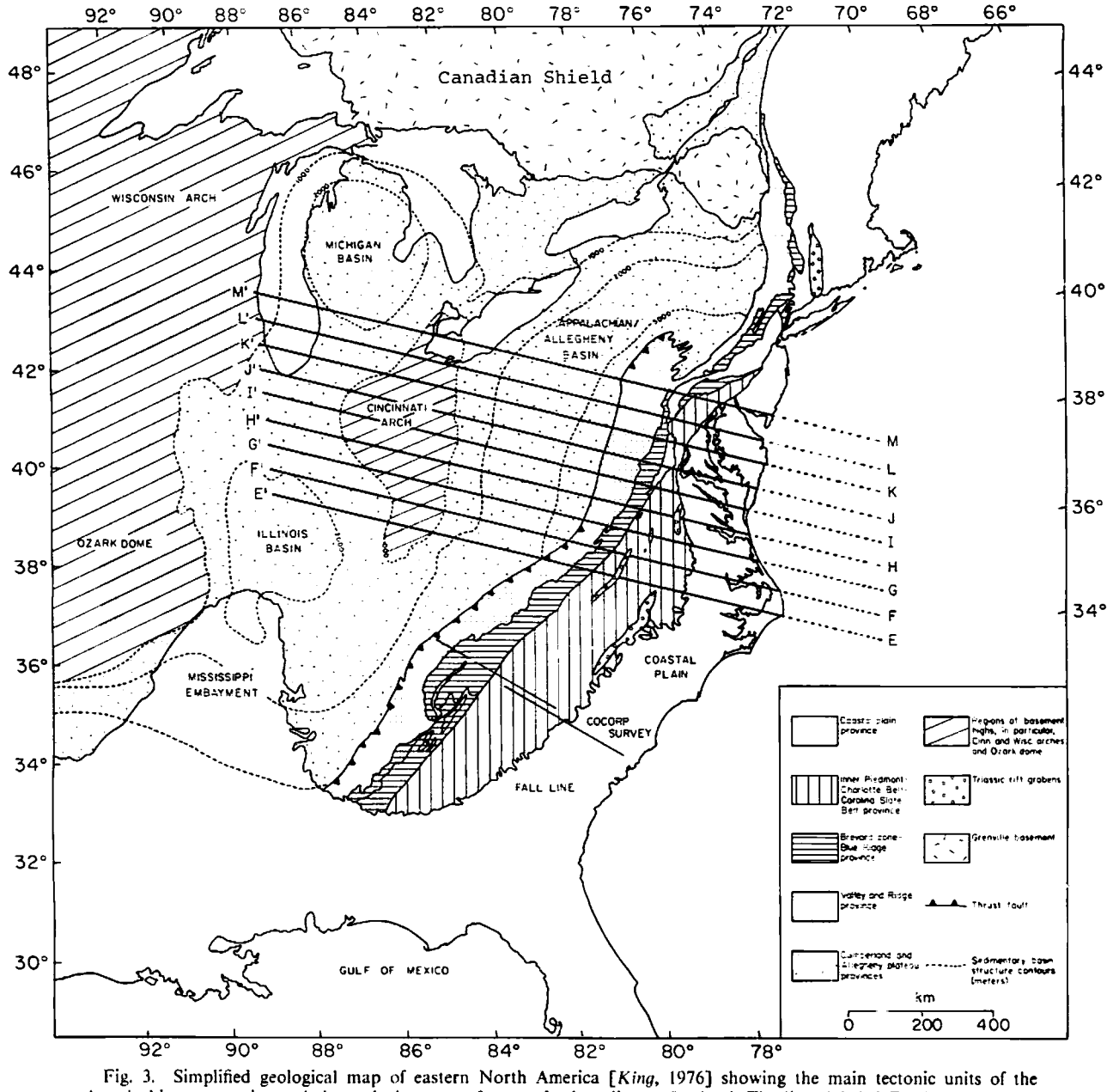


Fig. 3. Simplified geological map of eastern North America [*King*, 1976] showing the main tectonic units of the Appalachian mountains and the main basement features in the adjacent foreland. The lines labeled E–M represent the position of projected gravimetric and topographic data shown in Figure 6. Again, data exist only where the projection line is solid.

*Appalachians*

The Appalachian fold belt (Figure 3) has had a long geological history that began with the development of a passive continental margin during late Precambian to Early Ordovician time. During middle-late Paleozoic (Devonian to Permo-Carboniferous) there were major collisional events resulting in the characteristic fold and thrust belt of the Appalachians.

The geology of the southern Appalachian fold belt can be subdivided into four main tectonic provinces. the Piedmont, the Blue Ridge, the Valley and Ridge, and the Cumberland and Allegheny [e.g., *Hatcher*, 1981]. The Piedmont consists of repeatedly deformed metamorphic rocks, the main subdivisions of which are the Carolina slate and Charlotte belts, synorogenic to postorogenic granite plutons, and scattered occurrences of ultramafic rocks. The age of the main deformation and metamorphism is Ordovician/Silurian (Taconic Orogeny), while the age of the postorogenic granites is late Paleozoic. The Blue Ridge province, which is separated from the Piedmont by the Brevard Zone, consists of thrust sheets of reworked Precambrian basement (Grenville province), metamorphosed Precambrian and lower Paleozoic cover rocks, and minor occurrences of ophiolites. The Valley and Ridge province consists of unmetamorphosed cover sediments of Cambrian to Carboniferous age which have been involved in low-angle thrusting and nappe formation [*Hatcher*, 1981]. The Cumberland and Allegheny plateaus, which are separated from the fold belt by the Allegheny front (Logan's line), represent the flexural foreland basin of the Appalachian fold belt. The basin is asymmetric, ~7 km in thickness and varies in width from 200 to 400 km with respect to the Allegheny front. The Allegheny front in the southern Appalachians overrides

the foreland basin (in the vicinity of Knoxville, Tennessee) in a manner similar to the thrusting of the sub-Himalayas over the Ganges Basin. The main phase of foreland basin development was during the Devonian-Carboniferous following the Taconic orogeny (Silurian/Ordovician). The foreland sediments progressively onlap basement rocks of the Cincinnati arch.

## TECTONICS

The collisional events within mountain ranges are recorded in the sediments and basement structure as thrust and nappe formation (thin skin tectonics), basement reactivation and crustal faulting (thick skin tectonics), and regional metamorphism. Consortium for Continental Reflection Profiling (COCORP) seismic reflection profiling within the southern Appalachians has shown the existence of large-scale overthrusting of major allochthonous sheets along a low-dipping master decollement [*Iverson and Smithson*, 1982; *Harris and Bayer*, 1979]. This suggests that the entire Blue Ridge and Piedmont provinces constitute an allochthonous sheet, 6–15 km thick, thrust at least 250 km over an autochthonous Palaeozoic continental margin [*Cook et al.*, 1979]. Thus mountain building may well be dominated by horizontal compressive forces [e.g., *Rodgers*, 1970; *Brown et al.*, 1981]. Furthermore, present-day seismicity patterns [*Seeber and Armbruster*, 1981] suggest that the ancient decollement surface may easily be reactivated by later plate readjustments.

The timing of continental collisions is usually identified by the renewal/initiation of thrusting, folding, and metamorphism associated with an orogenic event. For example, the Acadian and Alleghenian orogenies of the Appalachians result from the collision and emplacement of displaced terrains onto the North American craton, as evidenced by palaeomagnetic data [*Kent and Opdyke*, 1978, 1979; *Van Der Voo and Channell*, 1980]. These displaced terrains may represent microcontinents, island arcs, or ophiolites associated with the destruction of oceanic basins [*Hatcher and Odom*, 1980]. The master decollement over which these displaced terrains were obducted is preserved as either a suture or cryptic suture. Suture zones represent the position of the destruction of oceanic lithosphere and the consequent juxtaposition of continental blocks [*Dewey*, 1976, 1977]. Repeated continental collision may lead to a protracted history of thrust emplacement. For example, the Ivrea body of the western Alps appears to have been emplaced into intermediate crustal levels at the end of Hercynian time, later to be reactivated by the Alpine orogeny and thrust to the surface [*Schenk*, 1981]. The repeated obduction of displaced terrains, therefore, tends to reactivate preexisting thrust and normal faults, redistributing the mass of allochthonous material loading the basement [*Beaumont*, 1981].

Continental blocks or flakes may be produced during the attempted subduction of continental lithosphere [*Oxburgh*, 1972; *Shackleton*, 1981; *Soper and Barber*, 1982]. The size of the resulting flake is probably dependent on the infrastructure of the subducted crust. In Europe, detailed seismic studies of both the crust and upper mantle show the existence of low-velocity channels which may also act as low-strength zones [*Mueller*, 1977; *Giese and Prodehl*, 1976]. These low-velocity channels, which typically exist at 10–15 and 24–28 km in the European upper crust [*Mueller et al.*, 1980], may be localities for crustal decoupling and flake generation during continental collision [*Oxburgh*, 1972; *Hsü*, 1979]. In the Himalayas, however, there is a lack of detailed seismic studies, and so details of the crustal and upper mantle structure are poorly known.

## CRUSTAL STRUCTURE

The transfer of mass associated with mountain building should be detectable seismically by variations in crustal velocities and thicknesses. For example, continental flexure should result in the deflection of individual crustal layers and the M discontinuity, and therefore not only will there be an associated Bouguer anomaly but also a change in crustal thickness.

### *Himalayas*

Surface wave studies [*Gupta et al.*, 1982] suggest that the regional crustal thickness of the Indogangetic plain (Figure 1) is in the range 40–50 km. The crust consists of an upper 10–20 km thick layer of velocity of 5.9–6.1 km/s overlying a 20–30 km thick layer of velocity 6.6–6.8 km/s [*Bhattacharya*, 1971; *Chun and Yoshii*, 1977]. Furthermore, body wave studies [*Gupta et al.*, 1977] indicate that the crust of the Indogangetic plain underthrusts the Himalayas. The crustal thickness beneath the High Himalayas is not well known, but recent studies [*Teng et al.*, 1980] indicate approximately 50–70 km.

The average crustal thickness beneath the Tibetan Plateau (Figure 1) is 70–75 km [*Teng et al.*, 1980] based on long-range seismic refraction data. The crust consists of an upper sedimentary layer 4–5 km thick, an intermediate layer about 40 km thick with velocity of 6.0–6.2 km/s, and a lower low-velocity layer with velocity of 5.6 km/s [*Wang et al.*, 1982]. Rayleigh wave attenuation studies [*Bird and Toksoz*, 1977] suggest that the lower crust is partially molten and may correlate with the low-velocity layer in the crust. Furthermore, focal mechanism solutions [*Chandra*, 1978] and propagation characteristics of $P_n$ and $S_n$ waves [*Barazangi and Ni*, 1982], are consistent with northward underthrusting of continental lithosphere beneath the Tibetan plateau. The amount of underthrusting (as indicated by the horizontal extent of the underthrust plate) beneath the Tibetan plateau is controversial; either the underthrust plate extends beneath the entire plateau [*Powell and Conaghan*, 1973; *Seeber et al.*, 1981; *Barazangi and Ni*, 1982], or it extends only to the Indus suture zone [*LeFort*, 1975; *Molnar and Tapponier*, 1975; *Klootwijk*, 1981].

### *Alps*

The average crust beneath the Molasse Basin is 20–30 km, based on long-range seismic refraction data [*Kahle et al.*, 1976; *Mueller et al.*, 1980]. Beneath the upper sedimentary layer the crust typically has velocities of 6.1–6.8 km/s with an abrupt change to 8.1–8.2 km/s at the M discontinuity. The crust is characterized by low-velocity zones at depths of 10 and 28 km [*Mueller et al.*, 1980]. The crustal thicknesses progressively increase from the foreland to the Alps.

In regions of high topographic relief the crustal thicknesses increase to 40–50 km with a maximum crustal thickness of 50–60 km generally reached south of the Insubric line. As pointed out by *Giese et al.* [1982], *Rybach et al.* [1980], and others, a characteristic feature of the Alpine mountain system (the Pyrenees-Apennines-Carpathians-Dinarides) is the existence of an asymmetric crustal "root" beneath the mountains. In particular, the maximum crustal thickness is systematically displaced from the maximum topographic relief. Seismic cross sections of the area of maximum crustal thickness show a repetition of velocities defining the crust/mantle transition. This has been interpreted [*Cassinis et al.*, 1979; *Giese et al.*, 1982] as resulting from tectonically produced crustal "doubling" of the M discontinuity such as may be produced by obduction of crustal flakes.

The hinterland of the Alpine system (e.g., the Po Basin) is characterized by similar crustal thicknesses as underlie the Molasse Basin. Except for the upper most part of the crust (10 km), no fine-scale structure appears to exist within the hinterland crust [*Mueller et al.*, 1980].

*Appalachians*

There have only been a limited number of seismic refraction studies of the Appalachian system [*Pakiser and Steinhart*, 1964; *James et al.*, 1968]. The depth to the M discontinuity varies from about 30 km beneath the Atlantic coastal plain to about 40–50 km beneath the highest topographic relief. The crustal velocities range from 6.0 to 6.2 km/s [*Pakiser and Steinhart*, 1964], although the fine-scale crustal structure is not well known. The available evidence suggests, however, a lack of present-day low-velocity zones within the crust [*Prodehl*, 1977]. The region of thick crust appears to extend from the Appalachians [*Pakiser and Steinhart*, 1964] westward and underlie the continental interior of the midwestern United States [*Kanasewich*, 1966].

## Data Reduction and Description

We have used in this study gravity and topography data supplied by the U.S. Defense Mapping Agency (DMA), St. Louis, Missouri. Because of the large amount of data involved ($10^4$–$10^5$ stations in the study areas) we developed an efficient data storage and retrieval system on the Lamont-Doherty VAX computer system. This system (Appendix A) allows rapid access of the station data and enabled us to construct automatically gravity and topographic profiles across mountain ranges. Generally, mountain ranges can be represented as two-dimensional structures, and so we have therefore projected gravity and topography profiles normal to some "classically" defined linear feature that can be either a suture or major decollement surface within each mountain range: for the Appalachians it is the Brevard Zone, for the Alps the Insubric line and its equivalents, and for the Himalayas the main boundary fault.

Most previous gravity studies at mountain ranges have been based on "static" modeling of a single gravity anomaly profile [e.g., *Diment*, 1968; *Mueller and Talwani*, 1971]. Thus it is not clear whether the inferred crustal structure is representative of the entire mountain range. In this study, to be statistically representative, we have used 6–12 profiles from each mountain range and attempt to find a model that takes into consideration the mechanical properties of the lithosphere and gives an acceptable fit to the observed gravity anomalies over each mountain range.

Recently, attempts have been made to remove statistically the bias introduced by a single profile in the continents by using admittance function techniques [*Dorman and Lewis*, 1971; *McNutt and Parker*, 1978; *Stephenson and Beaumont*, 1980; *McNutt*, 1980]. There are two major problems, however, with applying this technique to continental regions. First, the technique implicitly assumes that the surface topography represents the only load acting on the continental lithosphere; and second, because of the use of a two-dimensional Fourier transform the admittance technique necessarily samples large geographic areas, and thus it is not clear how the obtained admittance function relates to particular geological features.

We present in Figures 4, 5, and 6 the observed topography, free air gravity anomalies, and recalculated Bouguer gravity anomalies over the Himalayas, Alps, and Appalachians. The gravity and topography profiles (Figures 4, 5, and 6) range in length from 200 to 1200 km and include all available station data within a given "window" width (Appendix A). A simple Bouguer anomaly was calculated from the observed free air anomaly and topography supplied by DMA using a theoretical Bouguer admittance function such that

$$\Delta G(k) = G(k) - 2\pi\gamma\,\Delta\rho\,H(k) \quad (1)$$

where $\Delta G(k)$ is the frequency domain simple Bouguer anomaly referred to sea level, $G(k)$ the Fourier transform of the free air anomaly, $\gamma$ the gravitational constant, $\Delta\rho$ the Bouguer density (set to 2.67 g cm$^{-3}$), and $H(k)$ the Fourier transform of the topography, $h(x)$. This results in an internally consistant Bouguer anomaly. In order to stabilize the Fourier transform, we subtract a mean elevation from the topography so that the resulting simple Bouguer anomaly will have an artificial zero datum. By adjusting the datum of the calculated simple Bouguer anomaly data. Comparisons for the Alps (Appendix A) show that there are significant differences (20–30 mGal) only for short-wavelength ($\lambda \gtrsim 50$ km) topographic features. Therefore the simple recalculated Bouguer anomaly is adequate for studying long-wavelength gravity anomalies ($50 < \lambda < 1000$ km) associated with mountain ranges. Figures 4, 5, and 6 show that there is a close correlation between free air gravity anomalies and mountain topography, particularly for short wavelengths ($\lambda < 200$–$400$ km). At longer wavelengths the correlation is generally poor except on some profiles of the western Alps (profiles O–L), where a positive correlation is observed, and on some profiles of the central and eastern Alps (profiles D–G), where a negative correlation is seen. Because of the close overall correlation of gravity and topography, free air gravity anomalies show an extremely variable pattern over the three mountain ranges considered and relate to the rugged topography of these mountains.

The Bouguer anomaly over the Alps, Appalachians, and Himalaya, in contrast, shows a remarkably uniform pattern. The Alps consist of a positive-negative gravity anomaly "couple" (Figure 5). The minimum gravity anomaly is about 100–200 mGal in amplitude, is asymmetric, and varies in width from about 100 km in the western Alps to about 400 km in the eastern Alps. The gravity anomaly minimum correlates with the northern boundary of the crystalline and metamorphic rocks that form the central Alps. The maximum gravity anomaly is about 150–200 mGal in amplitude, is symmetric, and varies in width from about 100 km in the western Alps to >200 km in the eastern Alps. The gravity anomaly maximum correlates with the southern boundary of the crystalline and metamorphic rocks except in the eastern Alps where it correlates with the Po and Veneto molasse basins. There is no obvious correlation between the gravity maximum and the Insubric line; the maximum is located 10–50 km south of the line in the western Alps, while the maximum in the eastern Alps is located about 200 km south of the line. The Appalachian fold belt is also characterized by a similar positive-negative anomaly "couple" (Figure 6). The minimum gravity anomaly is about 50 mGal in amplitude and about 100 to 400(?) km in width. The Valley and Ridge province, which consists mainly of siliceous and calcareous cover sediments of Paleozoic age, correlates with the minimum gravity anomaly. The maximum gravity anomaly is 75–100 mGal in amplitude and is about 150–300 km in width and correlates with crystalline and metamorphic rocks of the Inner Piedmont. The profiles of the Himalayas, which generally do not exceed north of the Siwaliks, do not show this positive-negative anomaly "couple." Profiles traversing the entire

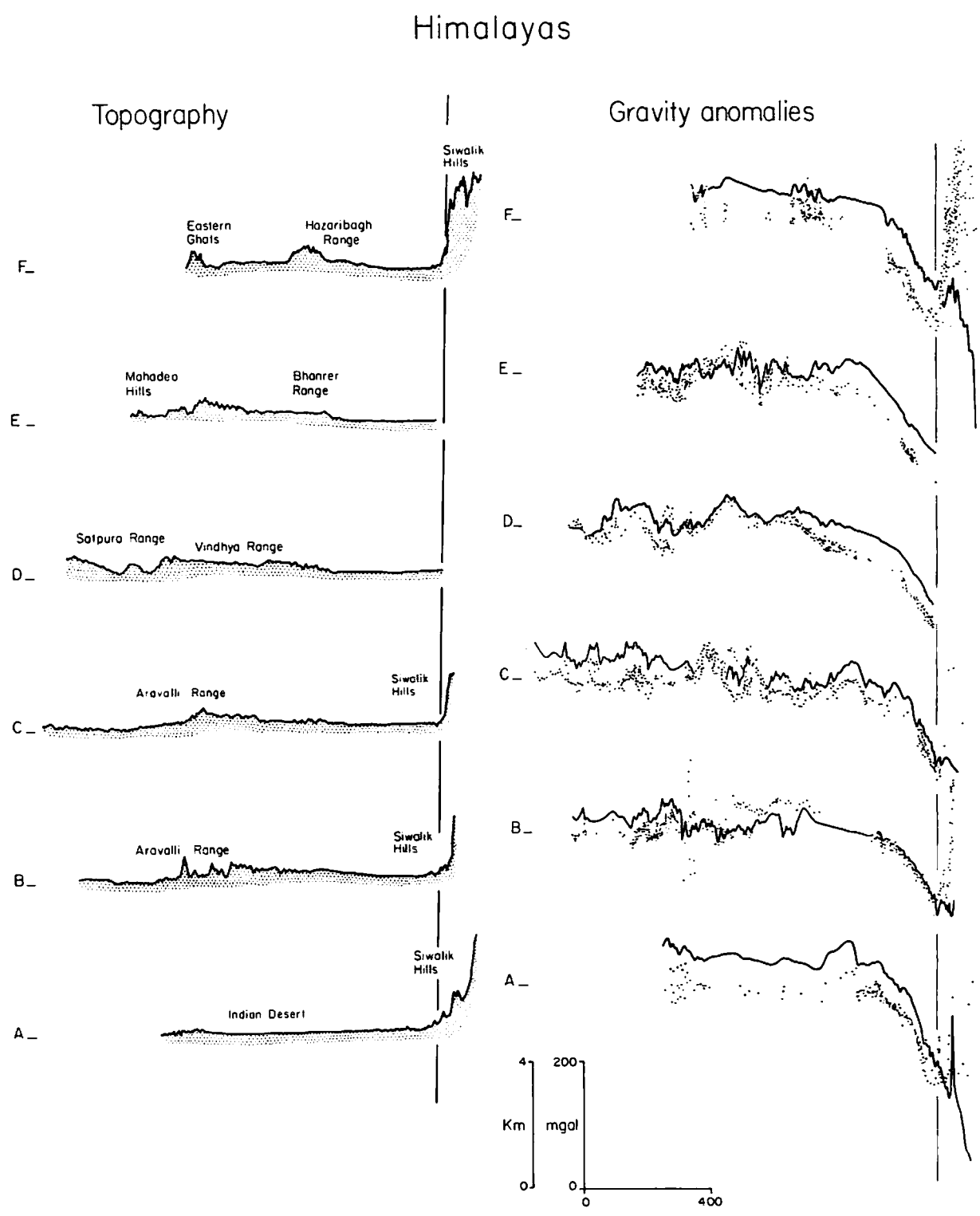


Fig. 4. Topography and gravity anomaly profiles across northern India and the Himalayan mountains. The dots indicate observed free air gravity anomaly values, and the solid line indicates the simple Bouguer anomaly. The profiles have been stacked on the minimum free air gravity anomaly which correlates with the Siwaliks. The Bouguer gravity anomaly is characterized by a long-wavelength ($\lambda \sim 400$ km) negative component which is related to the flexural loading of the Indian foreland basement.

mountain system (including the Tibetan Plateau) confirm the absence of a positive-negative anomaly "couple" in these mountains [*Wang et al.*, 1982]. The Himalaya profiles do show, however, an asymmetric negative gravity anomaly similar to the anomaly in the Alps and Appalachians. The gravity minimum is at least 100 mGal and may on some profiles exceed 400 mGal.

Classical models of isostasy would predict an inverse relationship between Bouguer anomaly and topography. Although this is the case of the eastern Alps, it is not true for the

Appalachians (Figure 7) or the western and central Alps. Since it is possible to correlate the positive Bouguer anomaly from the Ivrea Zone of the western Alps through to the eastern Alps, we suggest that this anomaly has a common origin. We do not imply that the Ivrea Zone itself extends from the western to the eastern Alps but that the positive anomaly is related in some way to the obduction of detached crustal blocks from the overriding plate onto the lithosphere of the underlying plate during mountain building. Thus the observed inverse correlation between Bouguer anomaly and topography for the eastern Alps (Figure 7) may be fortuitous, since the southern gravity gradient may be related to the shape of these obducted blocks rather than the M discontinuity.

## FLEXURE OF THE CONTINENTAL LITHOSPHERE

The formation of mountain ranges is associated with the transfer of mass both horizontally and vertically. We would expect therefore that the continental lithosphere should respond by flexure to these applied loads. A number of previous studies have examined foreland basins in order to determine the role of flexure at mountain ranges [*Warsi and Molnar*, 1977; *Jordan*, 1981; *Beaumont*, 1981; *Turcotte and Schubert*, 1982]. They assumed, however, that the present-day and/or past reconstructed topography was the only load responsible for foreland basin formation, and therefore any effects caused by loads not represented by the topography (for example, major density variations within the foreland basin or underlying basement associated with mountain building) were not considered.

There is geological evidence [*Bally et al.*, 1966; *Walcott*, 1970; *Price*, 1973] relating the lateral migration of thrusts and nappes to foreland basin formation. The emplacement of thrust sheets and nappes onto the continental lithosphere constitutes a surface load which should deform the lithosphere by flexure. Associated with the loading, a flexural basin is produced, the amplitude and wavelength of which is characterized by the strength of the lithosphere. Figure 8 shows a flexural model in which the topography is the only load acting on the lithosphere. The schematic geological model summarizes the main features associated with surface loading: a load consisting of a stack of thrust sheets and/or nappes, reworking of the Molasse Basin sediments within the submolasse zone, prograding of the sediments toward the foreland, the development of a basement flexural bulge in the foreland, and the formation of an asymmetric basin with maximum depth under the load.

The free air and Bouguer gravity anomalies associated with surface loading are also shown in Figure 8. The Bouguer anomaly is characterized by an outer gravity high over the flexural bulge and an outer gravity low associated with the basement deformation under the surface load. The magnitude and wavelength of the Bouguer anomaly is dependent on the wavelength and height of the topography and the flexural rigidity of the lithosphere, respectively. The Bouguer anomaly (Figure 8) is similar in form to that observed over foreland basins of the Himalayas, Appalachians, and the Alps (Figures 4, 5, and 6). Further, the Bouguer anomaly over the Appalachians and Alps is characterized by an additional positive anomaly, suggesting that some form of load in addition to the surface topography is acting on the lithosphere.

The preservation of a molasse or flexural basin even when the associated mountain range has been significantly reduced by erosion (for example, the Appalachian during the Tertiary and the Alps during the Pliocene) suggests that loads, independent of surface topography, must act on the lithosphere. These loads could take the form of either density variations within the lithosphere or transmitted horizontal compression generated by the interaction of plates at their boundaries. Any load acting on the lithosphere will be associated with a positive gravity anomaly. The localized positive Bouguer gravity anomaly which characterizes the Alps and Appalachians (Figures 5 and 6) is unrelated to the topography and suggests the existance of local intracrustal loads.

During the formation of mountain ranges, obduction transfers mass (possibly as some form of crustal block or flake) from one plate to another, causing the basement beneath the obducted block to flex. In order to study lithospheric flexure at mountain ranges, however, it is necessary to develop a loading scheme which incorporates the various loads acting on the plates. Figure 9, which uses the theory presented in Appendix B to model the response of a broken plate to applied loads, summarizes the loading scheme adopted for this paper. Since thrusting appears to be an important tectonic process in mountain building, we assume that the obduction of crustal blocks initiates the loading process. The crustal block (Figure 9*a*) is supported by the flexural strength of the lithosphere and the buoyancy of the underlying material. However, the block cannot be fully accommodated within the flexural depression and therefore will always be associated wth significant topography (Figure 9*b*). We assume that the remaining depression is then iteratively infilled with sediment up to the predeformation surface (Figure 9*c*). As Figure 9*c* shows, even after sediment infills the depression, there still remains a significant crustal block topography. If this topography is eroded, then given sufficient time, the basement would be expected to rebound, resulting in the total destruction of the sedimentary basin and the crustal block. The observation that the peneplation of the Appalachians (in the Tertiary [*Johnson*, 1931]) and the Alps (in the Pliocene [*Trümpy*, 1973]) has not resulted in the destruction of their respective molasse basins suggests that a further load, in addition to the obducted block and surface topography, is acting on or within the lithosphere. The fact that this additional load, as identified by the positive Bouguer gravity anomaly, is not represented in the present-day topography implies that it must be in the subsurface. While we do not know precisely how the basement would rebound on unloading, we believe that it would return to the predeformation surface irrespective of any anelastic strains that may develop in the plate during loading. We refer to this load in Figure 9*d* as a subcrustal load even though it may have components within the lower crust.

Figure 10 shows the Bouguer gravity anomaly associated with the loading scheme in Figure 9 and the final mass configuration associated with Figure 9*e*. As with surface loading (Figure 8), there is an outer gravity low and high which is associated with the response of the basement to the applied loads. In addition, there exists an inner gravity high which is related to the subsurface crustal loads. The form of the Bouguer anomaly in Figure 10 is characterized by a positive-negative anomaly "couple." The negative component is strongly asymmetric and is related to the deformed basement, while the positive component is symmetric and is associated with subsurface crustal loads. This characteristic gravity anomaly pattern is strikingly similar to the gravity anomaly patterns observed in the Alps and Appalachians (Figures 5 and 6), suture zones within Proterozoic terrains [*Gibb and*

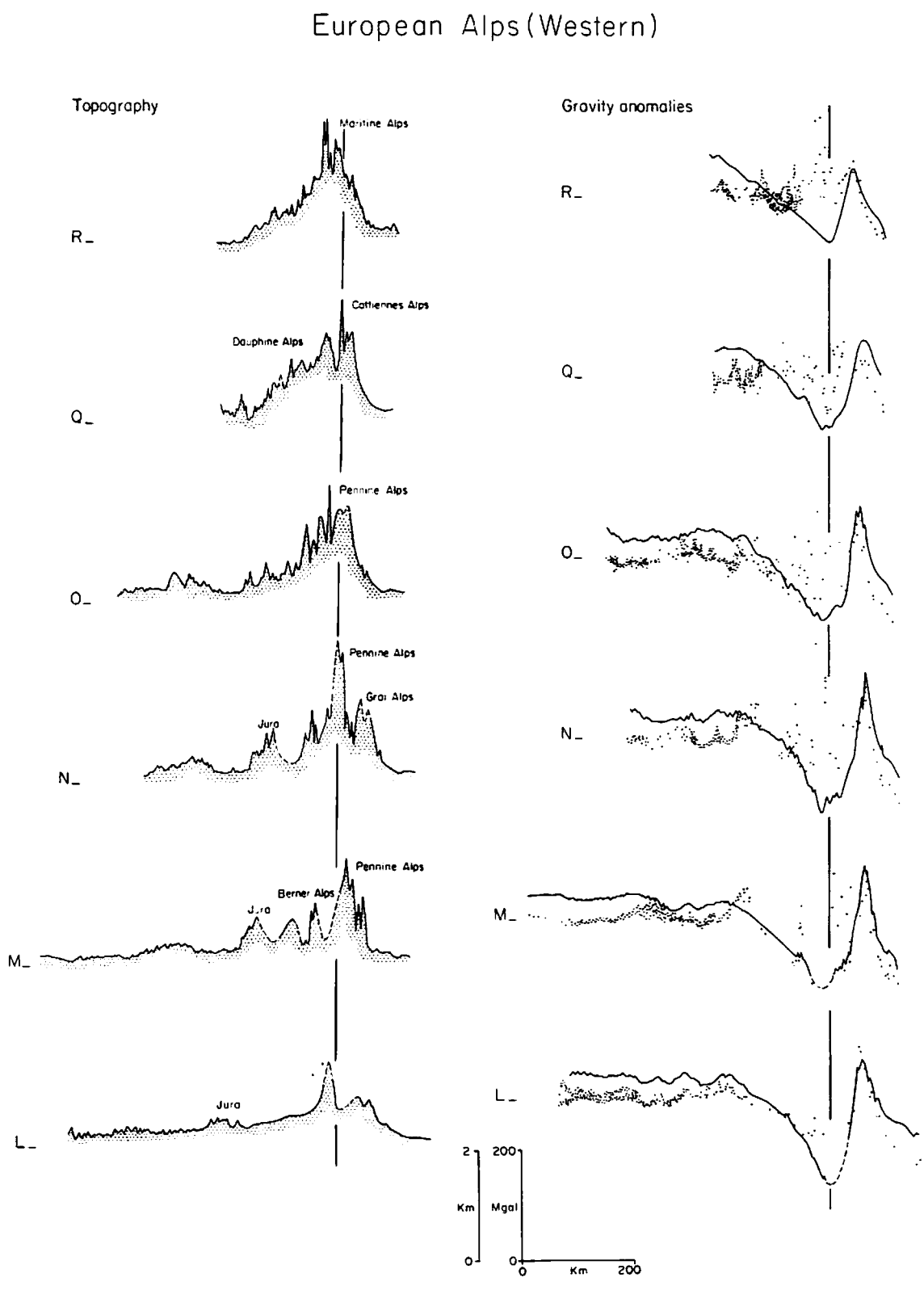


Fig. 5a

Fig. 5. Topography and gravity anomaly profiles of (*a*) the western Alps and (*b*) the central and eastern Alps. The profiles have been stacked on the minimum Bouguer anomaly. Symbols as in Figure 4. The Alps are characterized by a symmetric positive Bouguer anomaly component and an asymmetric negative anomaly component which together form a "couple." Note that this couple appears to be a correlatable feature from the western to the eastern Alps. The positive component is related to subsurface loads acting on the continental lithosphere, the response of which causes the long-wavelength negative component. In the west the positive anomaly is in part related to the Ivrea Zone. The apparent continuity of the gravity anomaly couple from west to east suggests a common origin for its existence.

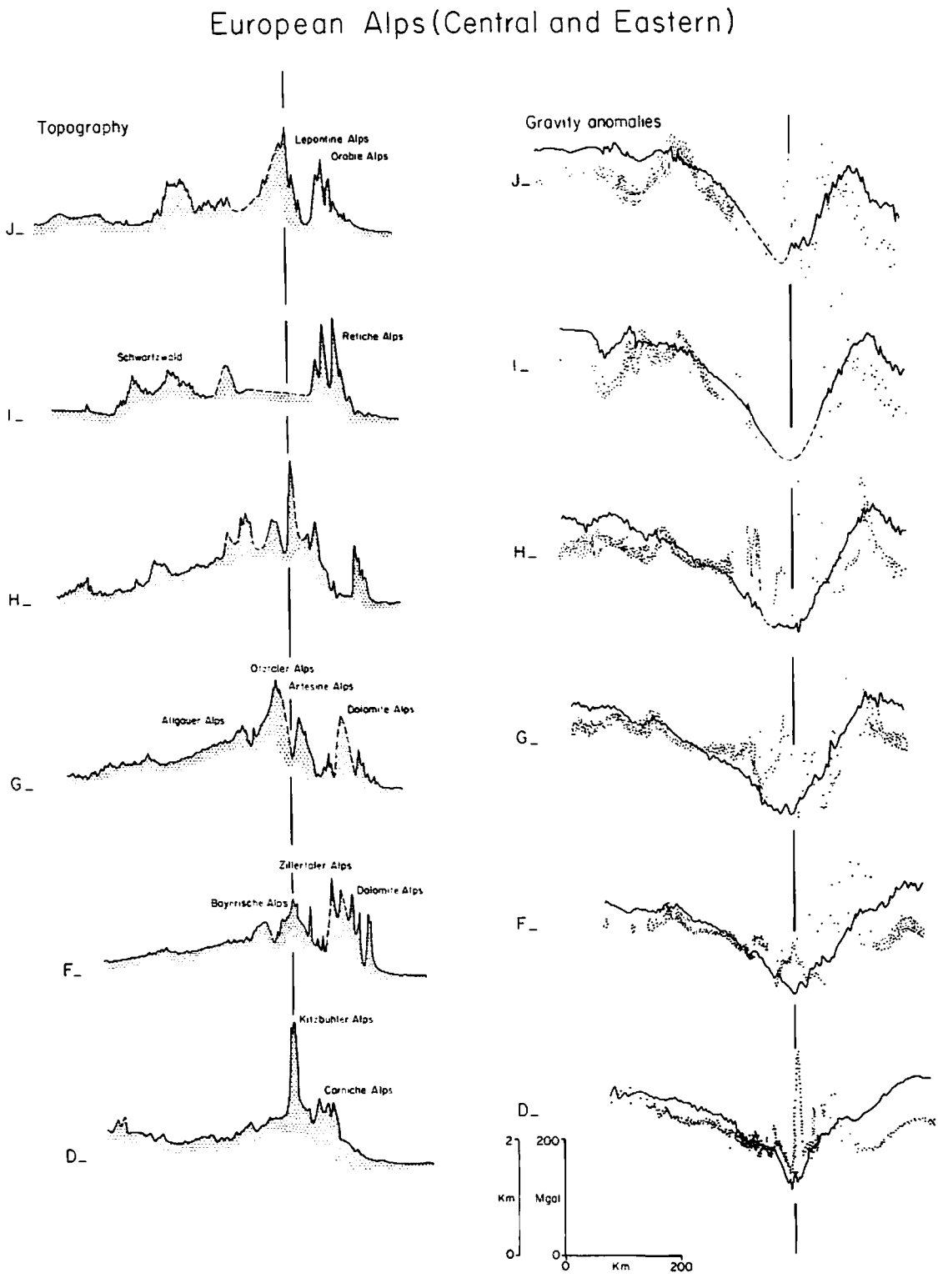


Fig. 5b

*Thomas*, 1976; *Tanner*, 1969; *Fountain and Salisbury*, 1981], and over deep-sea trench-island arc systems [*Watts and Talwani*, 1974]. For the Himalayas, however, the observed Bouguer gravity anomalies (Figure 4) [*Wang et al.*, 1982] appear to relate more to the characteristic pattern for surface loads (Figure 8). The loading within the Himalayas may therefore be more representative of the loading scheme of Figure 9*c* and suggests an explanation for the variation in the gravity anomaly patterns observed over orogenic belts. That is, the characteristic signature of the gravity anomaly over mountain ranges is dominated by the presence or absence of the subcrustal load.

In addition to plate-plate collisions causing the obduction of crustal blocks, the emplacement of these subsurface loads may directly cause the (re)mobilization of thrust sheets and nappes which compose surface topography. In particular, sur-

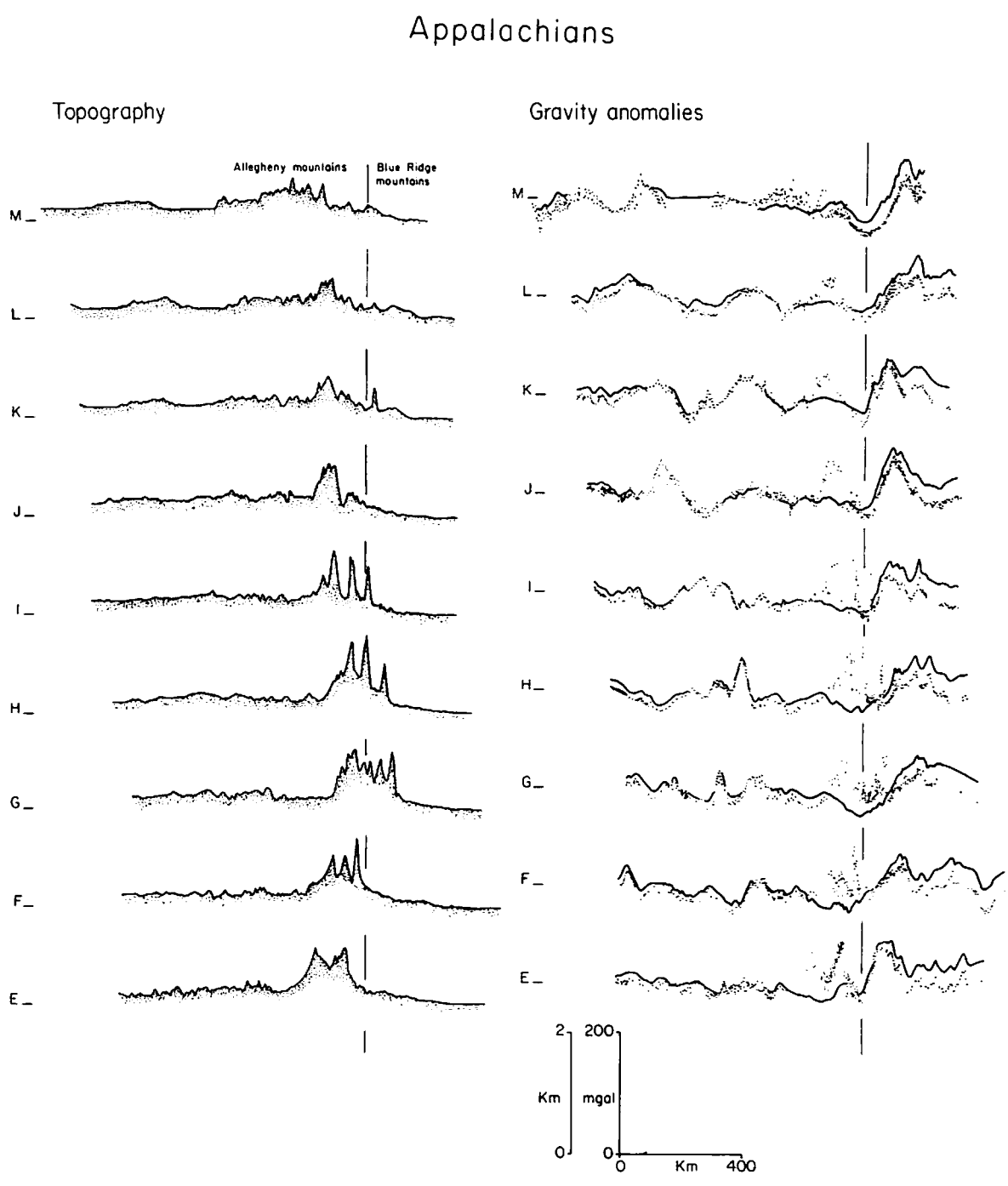


Fig. 6. Topography and gravity anomaly profiles of the southern Appalachian mountains and Allegheny/Appalachian Basin. The profiles are stacked on the minimum Bouguer gravity anomaly. As in the Alps, the Bouguer gravity anomaly is characterized by a positive-negative couple which is continuous for at least 600 km.

face topography will be produced between the obducted crustal block and the foreland (Figure 9). As shown in Figure 8, the surface topography is also a load, and so we must consider the combined effects of surface and subsurface loads if we are to understand the relationship between loading and foreland basin development. Figure 11 compares the effects of surface and subsurface loading.

A foreland basin will result from either surface or subsurface loads (Figures 8 and 11). When subsurface loads exist they will be the major control on both foreland basin formation and general crustal structure. Of lesser importance is the surface or topographic load, which should be associated with a local or secondary control on foreland basin development and crustal structure. The role of the surface load becomes increasingly important, however, as the strength of the lithosphere decreases.

Figure 12 shows the calculated free air and Bouguer gravity anomalies for combined surface and subsurface loading. We see that the characteristic positive-negative couple still exists and that the main effect of the surface load is to distort the flexural bulge associated with the subsurface loads and spread the deflection over a much greater area, in particular, into the foreland. The inner gravity high is necessarily unrelated to the topography. The resultant flexural basin has a width of ~400

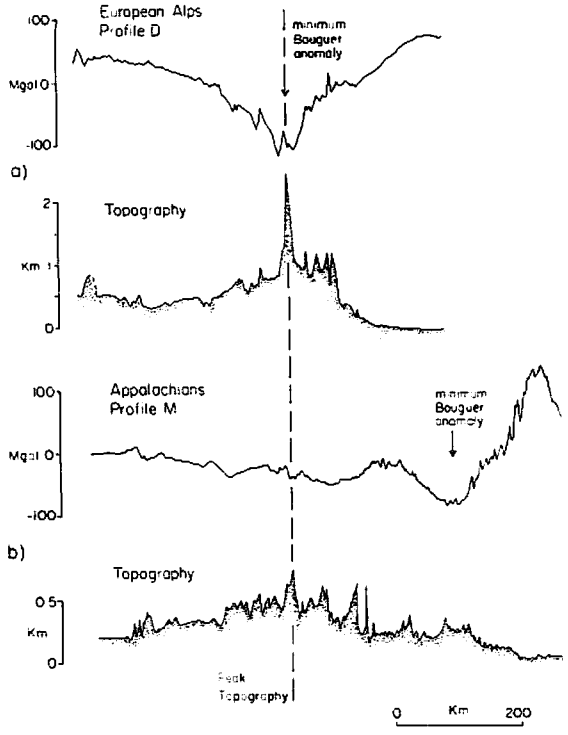


Fig. 7. Two representative topography and gravimetry profiles from the Alps and Appalachian mountains. Note that the minimum of the Bouguer anomaly is coincident with the peak topography in profile D of the eastern Alps (Figure 2) but is displaced from the topographic peak in profile M of the Appalachians (Figure 3).

km and maximum depth of ~20 km, though the maximum depth of the molasse basin defined from the submolasse zone (base of topographic load) is 5–7 km. The model predicts that for a standard 30-km crustal thickness in the foreland, the crustal thickness under the subsurface loads will be ~50 km. The maximum crustal thickness is not coincident with the maximum height of the topography, and so the crustal structure would be expected to be characterized by an asymmetric root displaced systematically from the maximum height toward the hinterland.

## METHODOLOGY

A major problem in understanding the role of flexure at mountain ranges is in determining the nature, distribution, and emplacement history of all the loads acting on the continental lithosphere. It is necessary therefore to use the free air gravity anomaly to obtain information about these loads. We will outline in this section the procedures used in this study to determine the characteristics of the various loads and their effects.

### *Mass Estimates of the Loads*

The emplacement of loads on the lithosphere represents the transferral of mass and, as such, will be associated with a mass anomaly. The obduction of crustal blocks appears to result in a mass excess, as evidenced by the large-amplitude positive Bouguer anomalies (for example, Figure 7). By using Gauss's theorem, it is possible to estimate the "effective mass" of the subsurface load, viz.,

$$\Delta M = (2\pi\gamma)^{-1} \int_s \Delta g \, ds \tag{2}$$

where $\Delta g$ is the free air gravity anomaly and $s$ the surface area represented by the anomaly. Since we have assumed two dimensionality for the mountains, $\Delta M$ is expressed as mass/unit length. We used the shape of the positive Bouguer anomaly to estimate $\Delta M$ for each of the mountain ranges. Estimates of $\Delta M$ range from $1 \times 10^{12}$ g cm$^{-1}$ for the western Alps to $4 \times 10^{13}$ g cm$^{-1}$ for the eastern Alps (Table 1). By assuming the density contrast $\Delta\rho$ between the load and the surrounding rocks (usually the infilling sediments of the flexural basin), $\Delta M$ can be used to determine the cross-sectional area of the load ($\Delta M = \Delta\rho \times$ load cross-sectional area). The emplacement of thrust sheets and nappes composing the surface topography also results in a mass excess which can be estimated directly from the form of the topography.

It would also be possible to estimate the mass of the surface load by considering the free air gravity anomaly of the mountains. However, since we can estimate the mass of the surface load directly from the topographic profile, it is not necessary to use (2).

### *Depth to Compensating Interfaces*

The principle of isostasy implies that the loads associated with mountain building will be compensated in some manner at depth. Unfortunately, there are too little seismic refraction data available to constrain the crustal and velocity structure of the compensating masses. We have therefore used the power spectrum of the observed free air gravity anomaly to estimate the mean depth to the compensating interfaces.

Consider the topographic variation, $h(x)$, along a single interface at mean depth, $z = d$ ($z$ positive down). By the Bouguer slab formula, the first-order gravity effect of the topographic variation measured on an observational plane at $z = 0$ is, in the frequency domain,

$$G(k) = 2\pi\gamma \, \Delta\rho e^{-kd} H(k) \tag{3}$$

where $k$ is the wave number, $\Delta\rho$ the density contrast across the layer, and $H(k)$ the Fourier transform of the topography $h(x)$. The power spectrum of $G(k)$ is simply

$$|G(k)|^2 = 4\pi^2\gamma^2\Delta\rho^2 e^{-2kd}|H(k)|^2 \tag{4}$$

However, (4) is associated with the gravity energy generated at only one depth. If we now consider the power spectrum due to a random distribution of compensating sources spread over a depth range $d \pm \Delta d$, the average gravity power spectrum $\langle|G(k)|^2\rangle$ is given by the ensemble average of each of the terms of the power spectrum, providing that $\Delta\rho$, $d$, and $H(k)$ are linearly independent. Then,

$$\langle|G(k)^2|\rangle = 4\pi^2\gamma^2\langle\Delta\rho^2\rangle\langle e^{-2kd}\rangle\langle|H(k)|^2\rangle \tag{5}$$

Now, $\langle e^{-2kd}\rangle = e^{-2k\bar{d}} \sinh(2k\Delta d)/k$, where $\bar{d}$ is the mean compensation depth. Taking the logarithm of the exponential component gives

$$\ln[\langle e^{-2kd}\rangle] = -2k\bar{d} + \ln[\sinh(2k\Delta d)/k] \tag{6}$$

which can be approximated as a straight line of slope $-2\bar{d}$. The factor $\langle e^{-2kd}\rangle$ is the dominating term of the power spectrum. Therefore for a discrete number of compensating masses the logarithm of the free air gravity power spectrum will show linear segments corresponding to each mass, the slope of which defines the mean depth to that mass.

Figure 13 and Table 1 summarize the mean depths of the compensating masses obtained from each of the mountain

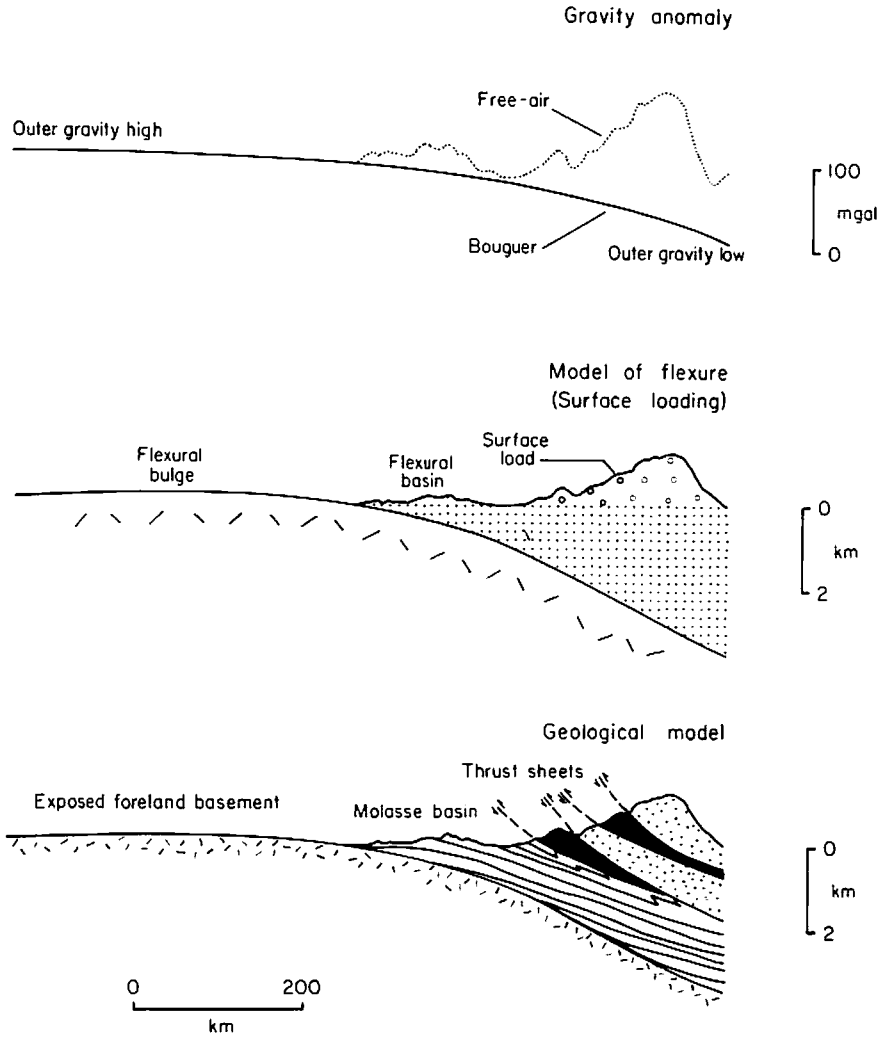


Fig. 8. Simple model for flexure of the lithosphere caused by the emplacement of a series of thrust sheet loads on the surface of the lithosphere. These loads result in the formation of a flexural or molasse basin and a flanking peripheral bulge in the foreland basement. The Bouguer gravity anomaly profile shows a long-wavelength asymmetric negative anomaly that correlates with the flexural basin and a long-wavelength small-amplitude positive anomaly that correlates with the bulge.

ranges. Figure 13 shows that the power spectrum consists of a number of linear segments, which can be interpreted in terms of the depth to the major density contrasts within the lithosphere. In particular, depth estimates appear to be related to the basement underlying the molasse basin ($d_3$), an intracrustal layer ($d_2$, possibly related to the major decollement surface along which obducted crustal block were emplaced), and the M discontinuity ($d_1$).

*Deflection Calculations*

The deflection of the lithosphere is the result of both surface and subsurface loading. If it is assumed that the flexural rigidity of the lithosphere is the same for both surface and subsurface loading, then Figure 11 demonstrates that subsurface loads are the dominating factor on the deflection and, as such, can be considered as the primary load in mountain development. The surface load therefore represents a secondary load and will have a more restricted effect.

We modeled the deflection of the lithosphere by the emplacement of obducted crustal blocks and subcrustal loads (both composing the primary load), subsequent sediment infill into the flexural depressions, and topographic construction by thrust sheet/nappe stacking and mobilization (the secondary loads). Specifically, our procedure is to begin with the primary loading events. The geometry of the loads inferred from the positive gravity anomaly were used to load a broken plate, assuming appropriate densities (Tables 1 and 2). We assumed that the edge of the broken plate, a distance $\Delta l$ from the toe of the obducted block, is coincident with the gradient of the hinterland positive gravity anomaly (Figure 12 and Table 2). The secondary loading event, represented by the emplacement of the surface topography, was superimposed on the equilibrium profile (equivalent to the predeformational surface) with a topographic offset, $\Delta t$, also relative to the edge of the broken plate (Figures 11 and 12 and Table 2).

The loading scheme outlined above assumes that the edge of the broken plate can be unequivocally determined from the observed inner gravity anomaly high (cf. Figure 10). In the case of the Himalayas, however, an obvious gravity high cannot be recognized. A recent gravity survey across the Tibetan Plateau [*Wang et al.*, 1982] has provided important constraints on the crustal and upper mantle structure of the region. The Bouguer gravity anomaly is characterized by an abrupt change in slope 200 km north of Mt. Everest (Figure

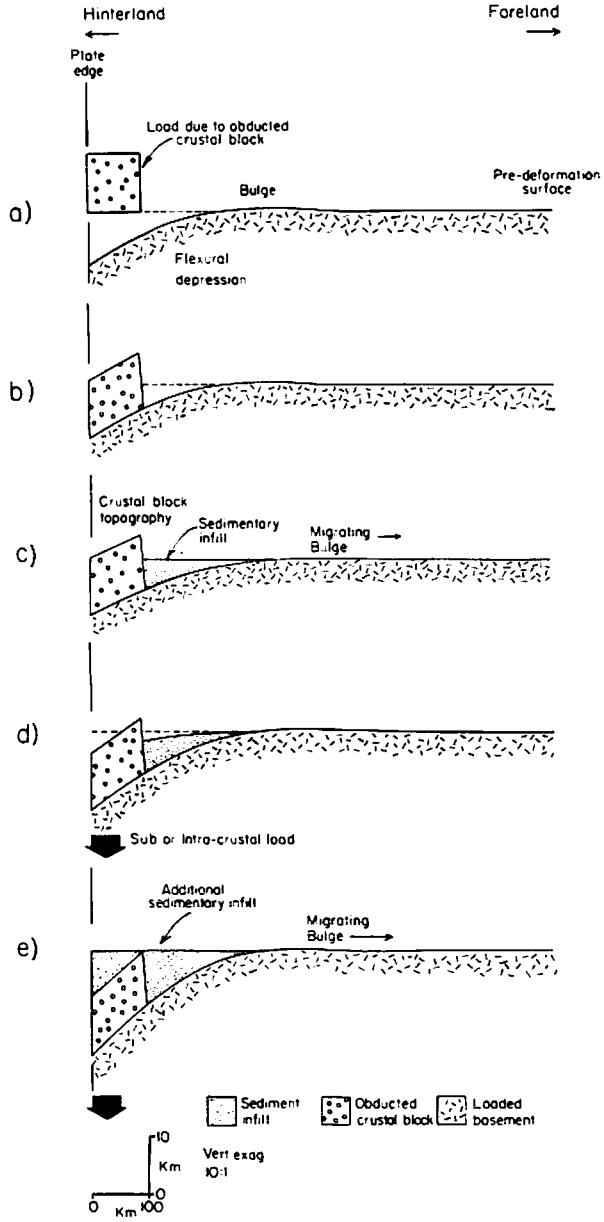


Fig. 9. The assumed loading scheme used in this study to describe the emplacement of loads onto the continental lithosphere at mountain ranges. The initial loading event is assumed to be associated with the obduction of a crustal block/flake onto the continental lithosphere. (*a*) As the lithosphere deforms, the crustal block/flake is partly accommodated within the flexural depression. (*b*) Sediment infilling of the depression results in further deformation of the lithosphere. (*c*) However, to maintain isostatic equilibrium, the crustal block is associated with significant surface topography. During erosion of the mountain topography, the lithosphere will rebound over a broad region, resulting in the eventual destruction of the foreland basin. The presence of foreland basins (and buried obducted blocks/flakes in mountain ranges), even though the topography has been destroyed by denudation, demands the presence of additional subcrustal or intracrustal loads. (*d*) These loads would result in further depression of the lithosphere and sedimentary infilling and allow for greater accommodation of the crustal block/flake within the flexural depression. (*e*) Isostatic equilibrium is achieved provided the subcrustal or intracrustal loads are maintained. Cases in Figures 9*c* and 9*d* are believed to be representative of the Himalayas and Alps/Appalachians, respectively.

14). The steep gravity gradient to the south of the Indus-Tsangpo suture suggests a model in which the load south of the suture is flexurally supported by the strength of the lithosphere, whereas north of the suture the load may be supported either by the lithosphere or possibly by dynamic forces related to Recent volcanism and present-day rifting of the Tibetan Plateau. The exact nature of this support, however, is unclear. The southern gravity gradient is well explained by the flexture of a broken elastic plate, the edge of which exists at the Indus-Tsangpo suture.

### *Estimation of the Effective Flexural Rigidity of Continental Lithosphere*

The gravity anomaly is sensitive to the long-term mechanical strength of the lithosphere. Since we have determined the geometry and mass of the emplaced loads, the rigidity of the lithosphere remains the only free parameter. Therefore, by comparing the gravity effect of the combined surface and subsurface loads and the associated deflection with the observed Bouguer gravity, the flexural rigidity of the continental lithosphere can be estimated. In particular, special emphasis was given to matching the amplitude and wavelengths of the outer gravity low and high. Because of the geological complexities of mountain ranges and their forelands, however, we have made only an order-of-magnitude estimate of the rigidity.

Table 1 summarizes the estimates of continental rigidity for the Himalayas, Alps, and Appalachian mountains. We see that mountain ranges are characterized by high flexural rigidities which range from $10^{30}$ to $10^{32}$ dyn cm which are significantly

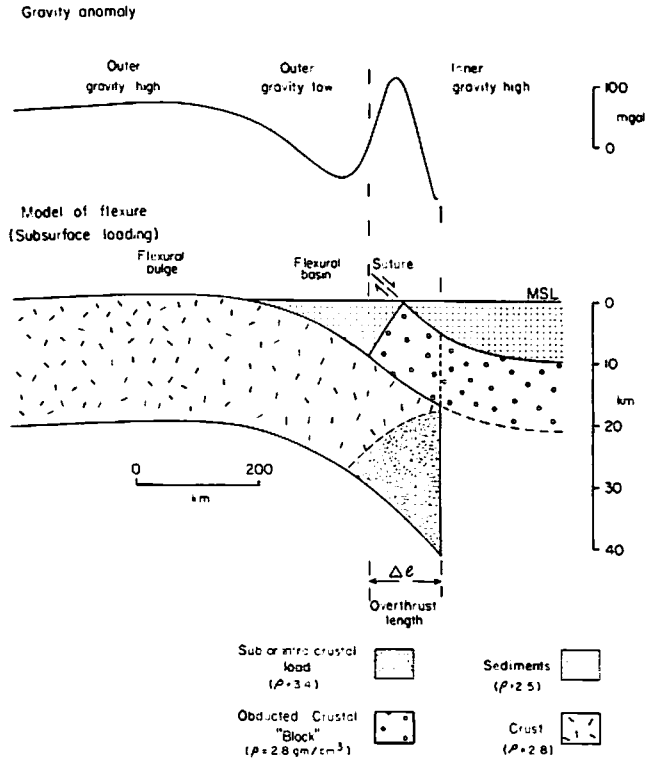


Fig. 10. Calculated gravity anomaly profile for the case in Figure 9*e*. Since there is no surface topography, the gravity anomaly represents either the free air or Bouguer anomaly. Note that the Bouguer anomaly profile, unlike the case for only surface loading, is characterized by a positive-negative couple in which the positive component is related to the buried loads, while the negative component is associated with the deformation of the basement.

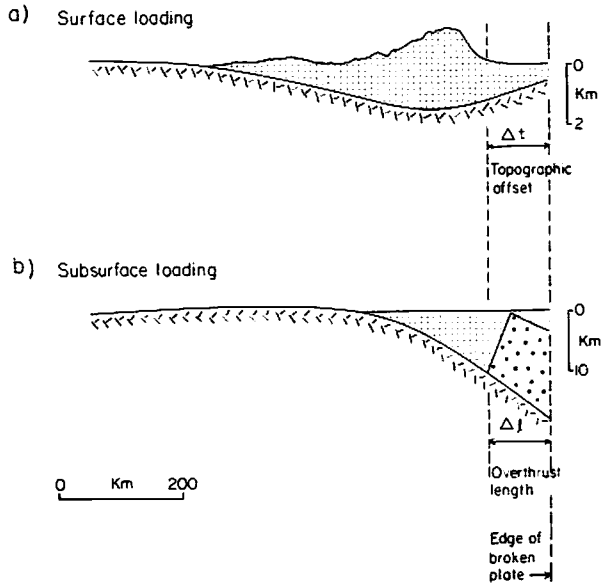


Fig. 11. Comparison of the flexural depressions and flanking bulges caused by (*a*) surface loading and (*b*) subsurface loading. The actual shape of the flexural curves depends on the flexural rigidity of the lithosphere ($D = 10^{30}$ dyn cm), the location of the surface topography in relation to the plate edge ($\Delta t = 100$ km), and the width of the overthrust length of the obducted crustal block/flake ($\Delta l = 100$ km). Note that the magnitude of the flexural depression and flanking bulges is significantly greater for subsurface than surface loading.

greater than estimates for the oceanic lithosphere [*Watts et al.*, 1982].

## RESULTS

We show in Figure 15 a comparison between calculated Bouguer gravity anomaly profiles for simple models of flexure and representative observed profiles from each of the mountain ranges. It was assumed that the subsurface and thrust/

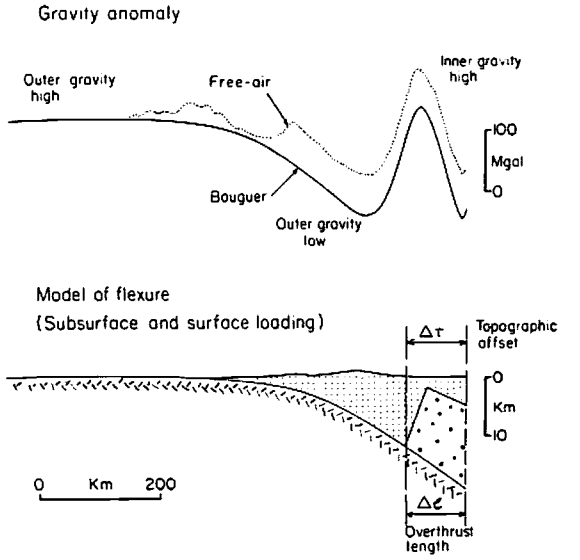


Fig. 12. Calculated gravity effect and flexure profiles for combined surface and subsurface loading. Note the existance of a well-developed positive-negative Bouguer anomaly couple. The positive anomaly corresponds to the buried subsurface loads, while the negative anomaly corresponds to the flexed basement. The effect of the surface loading, however, is to interfere with the flexural bulge of the subsurface loads, smearing the bulge further into the foreland.

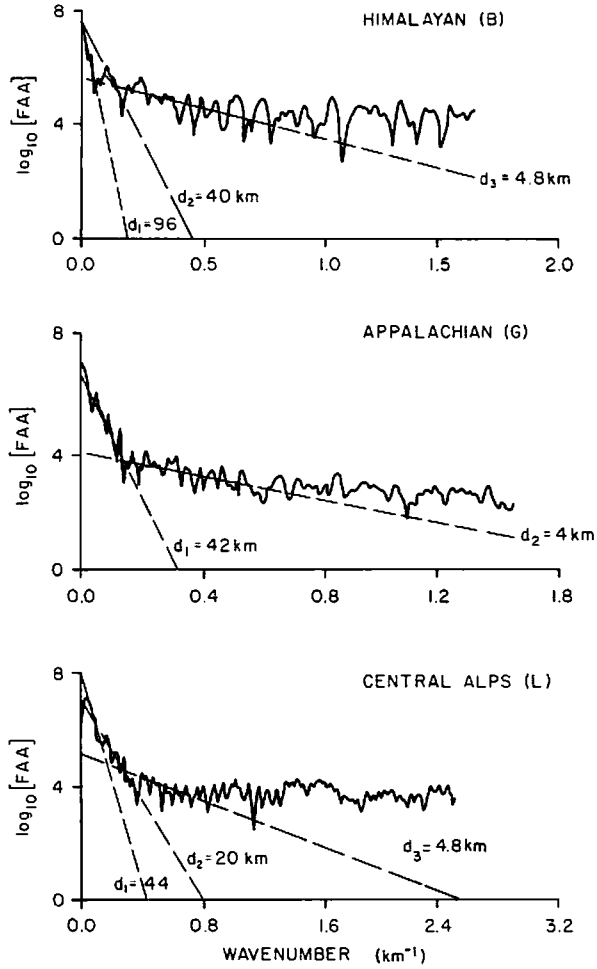


Fig. 13. Plot of wave number versus the logarithm of the free air gravity anomaly power for representative profiles of the Himalaya, Appalachian, and Alpine mountains. Linear segments of the power spectra suggest the existence of discrete density boundaries, the slope being an estimate of their mean depth. Superimposed solid lines on the power spectra represent a least squares fit to the observed linear segments. The gravity energy of these mountains appear to be associated with three main interfaces, $d_1$, the M discontinuity; $d_2$, an intracrustal layer; and $d_3$, the basement underlying the flexural basin.

nappe surface loads were emplaced onto a broken elastic plate. The overthrust length $\Delta l$ and topographic offset $\Delta t$ (Figures 10 and 11) were assigned from each mountain range (Table 2), and the effective elastic thickness $T_e$ was adjusted to best fit the gravity data from each mountain range (Table 1). For the Himalayas and Appalachians a single model was used to calculate the Bouguer anomaly. The close fit between observed and calculated anomalies over geographically widely separated profiles supports the statistical significance of the simple model. In particular, the loading of an elastic plate with uniform mechanical properties appears to be a satisfactory approximation for these mountain ranges since it explains a large proportion of the energy in the observed gravity anomalies. The best fitting elastic thicknesses for the Himalayas and Appalachians were 70–130 km. It is interesting to note that for both these mountain ranges the obducted crustal block and thrust sheet/nappes were emplaced on Archaean/Proterozoic-aged basement. In the case of the Alps it was necessary to increase the elastic thickness from 25 km in the western Alps to 50 km in the central and eastern Alps in order

TABLE 1. Model Calculations

| | Alps | Appalachians | Himalayas |
|---|---|---|---|
| Surface load mass, g cm$^{-1}$ | $2.8 \times 10^{12}$ | $2.2 \times 10^{12}$ | $\sim 4 \times 10^{13}$ |
| Subsurface mass, g cm$^{-1}$ | $1-4 \times 10^{13}$ | $1.2 \times 10^{13}$ | ... |
| Surface load depth of compensation, km | 20 | 42 | 80 (Tibet)<br>40 (Siwaliks) |
| Subsurface load depth of compensation, km | 44 | 42 | ... |
| Flexural rigidity, dyn cm | $10^{30}-10^{31}$ | $5 \times 10^{31}-10^{32}$ | $5 \times 10^{31}-10^{32}$ |
| Elastic thickness, km | 22.4–48.3 | 82.5–131.0 | 82.5–104.0 |

to fit the amplitude and wavelength of the outer gravity high and low (Figure 15). These Alpine elastic thicknesses are significantly smaller than the values obtained from the other mountain ranges. In the Alps, however, various loads were emplaced on Hercynian-aged (or Hercynian reactivated) basement, and we would therefore expect it to have, based on oceanic flexure studies [*Watts*, 1978], a correspondingly lower flexural rigidity than the older and hence cooler Archaean/Proterozoic-aged basements. The progressive eastward stiffening of the Alpine basement correlates with an observed decrease of present-day heat flow from western to eastern Europe [*Cermak*, 1979].

## Discussion

We have shown in this paper that the gravity anomaly "couple" observed over the Alps and Appalachians and outer and inner gravity signature of the Himalayas can be described by a model in which the continental lithosphere is deformed by flexure due to surface and subsurface loads emplaced during orogeny. In this section we examine the implications of this model for the crustal structure at mountain systems, admittance studies of the relationship between continental gravity and topography, and the long-term mechanical properties of continental lithosphere.

The close fit between the observed and calculated Bouguer gravity anomalies (Figure 15) demonstrates the applicability of the elastic plate model at mountain ranges. Implicit in the model is a prediction for the mountain crustal structure. By comparing the flexurally predicted crustal structure with that from the seismic refraction and reflection data, an independent test of the validity of the gravity-derived model can be made.

TABLE 2. Summary of Parameters Assumed in Calculations

| | Alps | Appalachians | Himalayan |
|---|---|---|---|
| Number of profiles | 12 | 9 | 6 |
| Profile window width, km | ±10 | ±5 | ±50 |
| Profile length, km | 400–660 | 1272–1347 | 920–1500 |
| Overthrust length $\Delta l$, km | 100–300 | 350 | 400 |
| Topographic offset $\Delta t$, km | 75–100 | 400 | 0 |
| | Value | | |
| $\rho$, g cm$^{-3}$ | | | |
| Topography | 2.7 | | |
| Sediment | 2.5 | | |
| Crust | 2.8 | | |
| Mantle | 3.4 | | |
| $E$, dyn cm$^{-2}$ | $10^{12}$ | | |
| $\sigma$ | 0.25 | | |
| $g$, cm s$^{-2}$ | 981 | | |

The elastic models (Figures 10 and 11) predict that the crust progressively thickens from the foreland to the region of the suture zone. Further, because much of the load is subsurface, we would not expect any obvious correlation between crustal thickness and topography. In fact, the maximum crustal thickness corresponds to the position of the obducted crustal block. In our mechanistic model we view that the obduction of this crustal block in turn leads to the development of the topography. We predict that the crust would rapidly thin across the suture zone (or its equivalent) toward the hinterland.

We present in Figure 16 a summary of geological and geophysical data along the Swiss geotraverse [*Rybach et al.*, 1980]. By comparison of the gravity model to the geological model we see that the general predictions of the flexural models are in good agreement with observations. In particular, the maximum crustal thickness is displaced toward the hinterland relative to the topography (Figure 16). Thus the flexural models generally explain the observations [*Giese et al.*, 1982] that the M discontinuity at mountain ranges is asymmetric and systematically displaced from the maximum topographic relief. The associated obduction of crustal blocks further predicts the existence of duplicated mantle velocities. In the flexural models the asymmetric crustal structure is a direct consequence of using a broken plate. The fact that there is an observed rapid crustal thinning across the suture zone (Figure 16) [*Giese et al.*, 1982] provides general support for

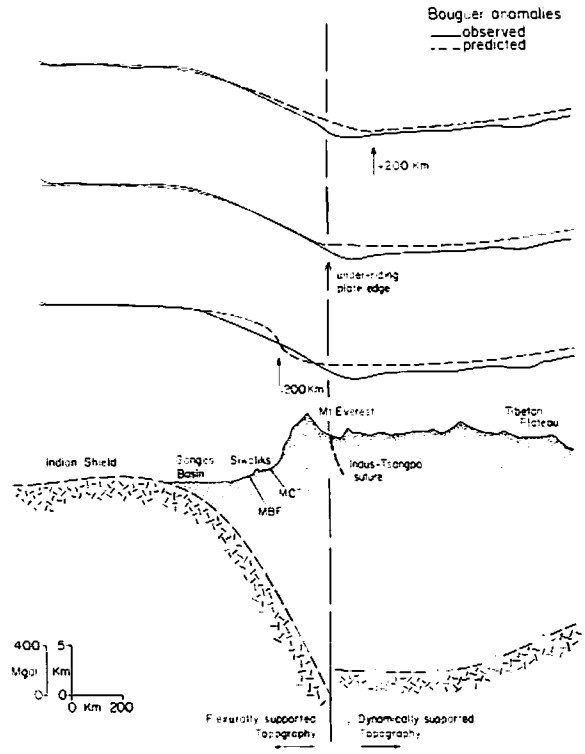


Fig. 14. Comparison of observed and calculated Bouguer gravity anomaly profiles of the Himalayas in the region of profile F (Figure 1). The observed anomaly is based on the work by *Wang et al.* [1982]. The calculated anomaly profiles have been computed assuming that the surface topographic load is the only load acting on the lithosphere and different positions of the plate edge in relation to the surface load ($\Delta t$, Figure 11). The best fit between observed and calculated anomalies is for the case where the edge of the plate coincides with the location of the Indus-Tsangpo suture (middle profile). Note that the amplitude and wavelength of the observed Bouguer anomaly can be explained by the simple flexure model.

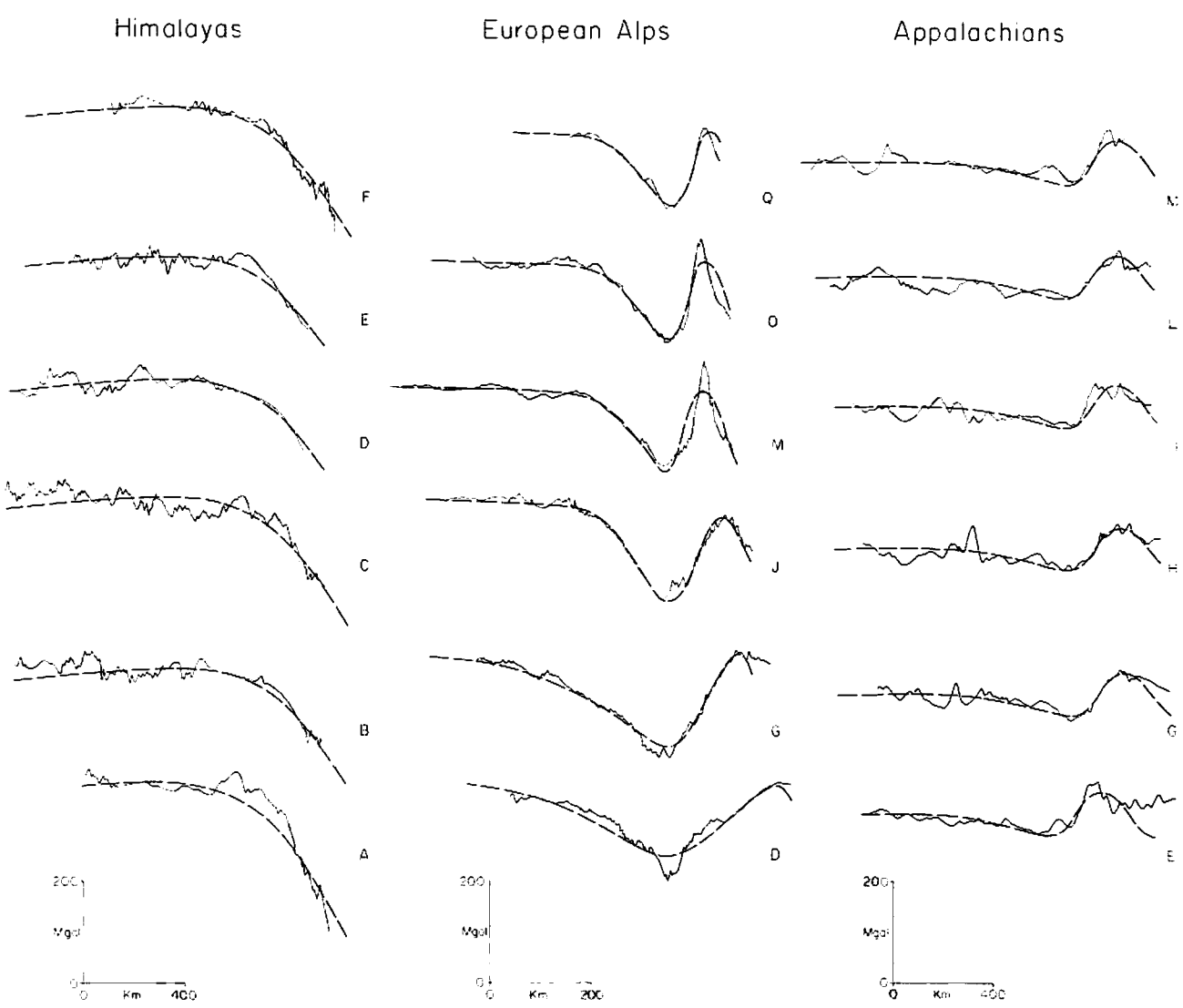


Fig. 15. Comparison of calculated and observed gravity anomalies for selected profiles of the Himalayas, Alps, and Appalachians. The solid lines are observed Bouguer anomalies and the dashed lines are calculated anomalies based on the simple flexure model with load sizes and flexural parameters as given in Table 2.

the existence of broken plates in characterizing the flexural response of mountain ranges. It addition, the crustal thinning associated with the underriding plate at the suture zone (Figure 16) may represent the subsurface load that maintains the flexural depressions of the molasse basins in the absence of surface loads (Figures 9*d* and 9*e*). The origin of this crustal thinning is unclear. For example, it may represent the crustal structure prior to loading of a rifted continental margin. Alternatively, this crustal thinning may be caused by back arc rifting processes associated with active subduction.

Figure 16 also shows the correlation between the observed Bouguer anomaly and surface geology. The inner gravity high is associated with the obducted crustal block of the Ivrea Zone and the crustal thinning, while the outer gravity low relates to the shape of the flexural depression. The crystalline massifs of the External Zone and the sediments of the Penninic Zone represent para-autochthonous/allochthonous material emplaced as a result of obduction of the Ivrea crustal block [*Hsü*, 1979]. Thus the deposition of molasse-type sediments is restricted to only a small and distant part of the total flexural depression. The progressive obduction of material causes the depocenter to migrate toward the foreland, as evidenced by the progressive onlap of sediments in the basin [*Clar*, 1973].

We have shown that the continental lithosphere is associated with relatively high effective flexural rigidities compared to those of oceanic lithosphere. It is somewhat surprising, therefore, that continental admittance studies using Bouguer gravity and topography data [*Lewis and Dorman*, 1970; *McNutt and Parker*, 1978; *Stephenson and Beaumont*, 1980] indicate that mountain topography is supported by plates with low flexural rigidities. This apparent contradiction can be reconciled if we consider that surface topography may not be the only load acting on the lithosphere in mountain ranges. We have shown that subsurface loads are a major contributor to the deflection of individual crustal layers and the M discontinuity. Thus the admittance technique necessarily predicts low effective rigidities because it assumes that only surface loads are responsible for the deflection which, in fact, is associated with both surface and subsurface loads. We have tested this hypothesis by calculating the admittance function for the 12 gravity and topography profiles of the Alps (Figure 5). By

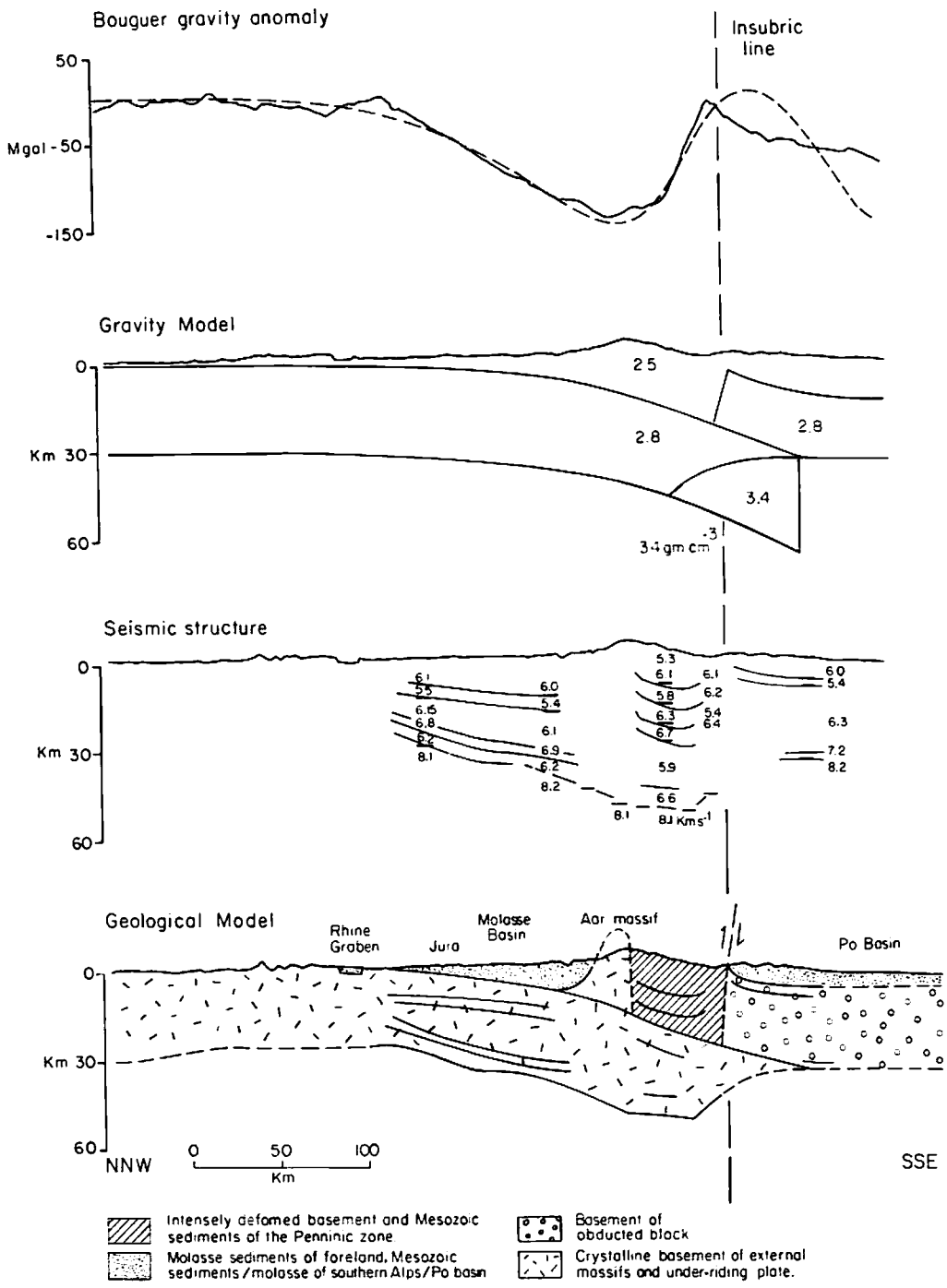


Fig. 16. Bouguer gravity anomaly, seismic structure, and gravity and geological models along the Swiss geotraverse [*Rybach et al.*, 1980]. The gravity model is based on the flexural scheme presented in this paper. In particular, three loads have been considered in deriving the deformation of the basement: the obducted crustal block ($\rho$ = 2.8 g cm$^3$), a subcrustal load ($\rho$ = 3.4), surface topographic load ($\rho$ = 2.7), and sediment infill ($\rho$ = 2.5). The geological model is a schematic cross section based on the gravity model and is generally consistent with previous regional geological interpretations [e.g., *Trümpy*, 1973].

comparing the resultant observed admittance to theoretical functions (based on models and assumptions used in previous continental admittance studies), we see (Figure 17) that the mountain admittance appears to require ridigities in the range $10^{27}$–$10^{28}$ dyn cm (cf. $10^{30}$–$10^{31}$ dyn cm). Therefore unless all the loads acting on the lithosphere are considered, the admittance approach significantly underestimates the actual rigidity of the continental lithosphere.

Lithospheric flexure is therefore an important phenomenon in continental tectonics, suggesting an alternative method of reducing continental free air gravity anomalies. In effect, the Bouguer reduction is a technique for "mass stripping" the gravity effect of mountains. However, it assumes an infinite flexural rigidity for the lithosphere and therefore does not adequately take into account the effect of the mountain's compensation on the gravity anomaly. It would seem that a more reasonable approach would be to mass strip the mountains flexurally and allow the lithosphere to have a finite rigidity.

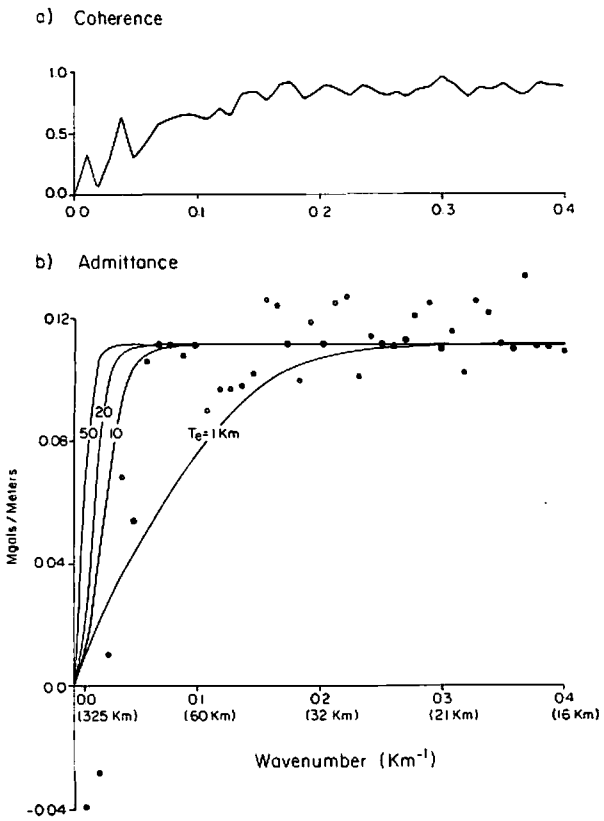


Fig. 17. The application of cross-spectral techniques to 10 free air gravity anomaly and topography profiles of the Alps. This technique assumes that the topography is the only load acting on the lithosphere. The amplitude of the admittance appears to be controlled by an elastic plate model with $T_e$ in the range 1–10 km ($10^{28}$–$10^{29}$ dyn cm). However, the coherence is unacceptably low for the wave numbers that are important in determining the isostatic model. The values of $T_e$ of 1–10 km are significantly smaller than the values estimated in this study (25–50 km, Table 1) so it appears that the admittance technique seriously underestimates the actual value of $T_e$.

The resulting isostatic anomaly removes the effect of both the topography and its compensation. This approach (Figure 18) successfully highlights the existence and form of a flexural "outer rise" in the European foreland.

There are a number of geological implications for a major role of flexure in the continents. The flexural rigidities that are obtained provide information on the long-term mechanical properties of continental lithosphere. We plot in Figure 19 the flexural rigidities from this study along with previously published rigidity values from oceanic lithosphere [e.g., *Watts et al.*, 1982]. As with the oceanic values, we reduced the continental rigidities according to the age of the continental lithosphere at the time it was loaded. For example, with the Alps the Eocene-Miocene (10–50 m.y.) loading [*Trümpy*, 1973; *Dietrich*, 1975] of Hercynian-aged (290–310 m.y.) basement (or basement thermally reset during the Hercynian orogeny) gives an age of the lithosphere at the time of loading of 240–300 m.y. Implicit in this calculation is that the Alpine orogeny did not thermally reset the underlying Hercynian-aged (radiometric) basement. Likewise, because of the observed large flexural rigidities associated with the foreland basement of the Himalayas and Appalachians, the orogenies forming these mountains did not thermally reset their underlying basements (Proterozoic and Grenvillian radiometric ages, respectively) either. However, it is clear that in some cases [*Miyashiro et al.*, 1982] an orogeny which is characterized by high-temperature regional metamorphism and extensive basement reactivation (e.g., the Grenvillian and Hercynian orogenies) tends to reset thermally its underlying basement. Thus it would appear that there are two broad types of orogenic processes that can affect the thermal structure of the continental lithosphere; the rigidity at the time of loading reflects the thermomechanical behavior of continental basement involved with these orogenies.

Figure 19 shows that there is a systematic increase in the flexural rigidity of the lithosphere with increasing lithospheric age at the time of loading. The continental values obtained in this study appear to be satisfactorily explained in a similar way as the oceanic values. Thus in an analogous way to the increase of flexural rigidity of oceanic lithosphere with age from a mid-ocean ridge, so does the flexural rigidity of continental lithosphere appear to increase with age. It would seem reasonable therefore that following a heating event within the continent, the rigidity may be reset (but not necessarily to zero) and would subsequently increase with age.

We suggest that continental lithosphere responds to applied loads, such as those developed during orogeny, by flexure over broad regions flanking mountain ranges. Figures 20–22 illustrate the expected position of the first flexural node ($y_b = 0$, equation (B9)) flanking the Himalayas, Alps, and Appalachians based on the rigidity estimates of this study. There is a close correlation between the position of the flexural node and the foreland limit of the molasse basin and between the outer rise and basement "swells" and/or "arches." There is a particularly close correlation between the position of the Cincinnati arch, Nashville and Jessamine domes, and Algonquin axis with the flexural outer rise.

The Cincinnati arch and related domes and arches have had a major control on the deposition of stratigraphic sequences in the continental interior of eastern North America. Geological evidence [*Wilson and Stearns*, 1963; *Rudman et al.*, 1965] suggests that these basement structures primarily influenced Cambrian and Ordovician sedimentation but also acted as zones of structural control in later Paleozoic time. This suggests a possible link between basement arches and the superposition of loads associated with the Cambrian passive margin and loads developed during the Ordovician/Silurian Taconic orogeny. In particular, the proto-Cincinnati arch may have been associated with a flexural bulge that developed inland of the Cambrian passive margin sedimentary sequence. Later orogenic events superimposed additional loads in the form of thrust sheets and nappes. The decollement associated with this obduction may be controlled by the position of the margin's hinge zone. This hinge zone may act as a "ramp" during deformation [*Watts and Steckler*, 1979; *Watts*, 1981] thereby concentrating these loads in the vicinity of the passive margin loads. The present-day basement configuration of the Cincinnati arch and related basement features may therefore be a result of the interference of flexural bulges associated with multiple loading events. Furthermore, the variable nature of the western boundary of the arch may be related to the interference of flexural bulges associated with the sedimentary loading within the Michigan and Illinois basins and the Mississippi embayment.

The flexural bulge is associated with tensional bending stresses above the neutral surface of the loaded plate. The position of the maximum bending stress caused by the primary and secondary loads exists between the first flexural node and the load. Figure 21 shows that there is a correlation between the position of maximum bending stress and the reac-

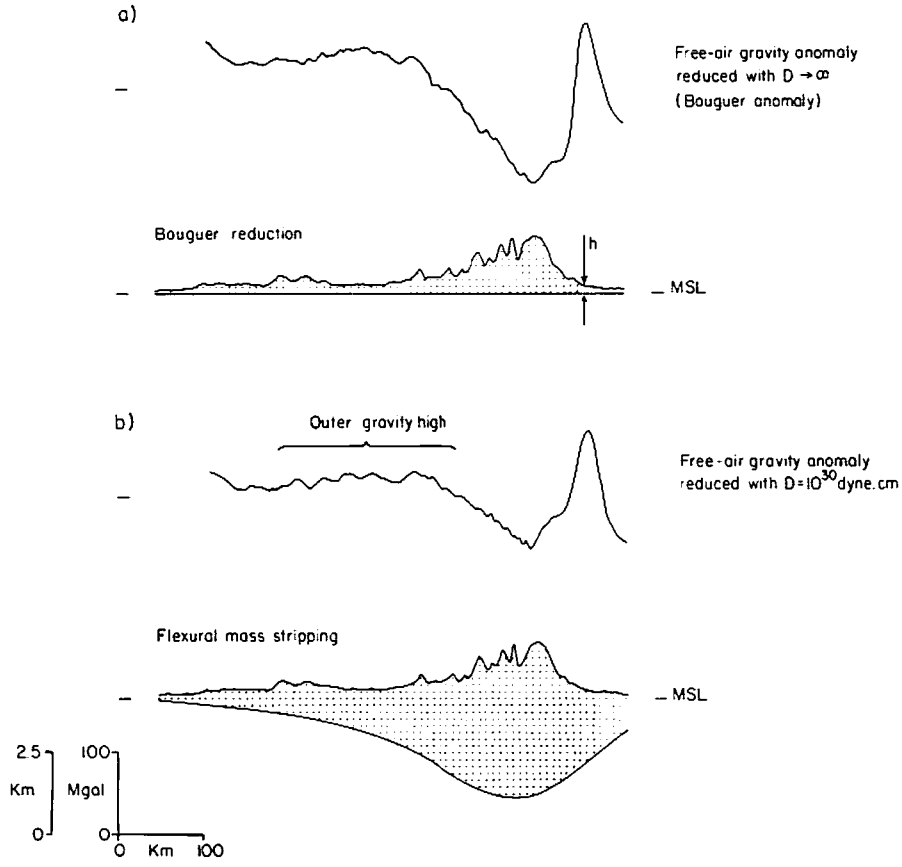


Fig. 18. Comparison of Bouguer anomaly profiles for the western Alps (profile O, Figure 5*a*) based on (*a*) the simple Bouguer reduction, which in effect assumes an infinite rigidity for the plate, and (*b*), a flexural "mass-stripped" profile, which assumes a finite rigidity for the plate and therefore includes a correction for the deformation of the plate due to the topography. Note that the flexurally mass-stripped profile tends to emphasize the flexural features (outer rise, flexural depression) associated with subsurface loading.

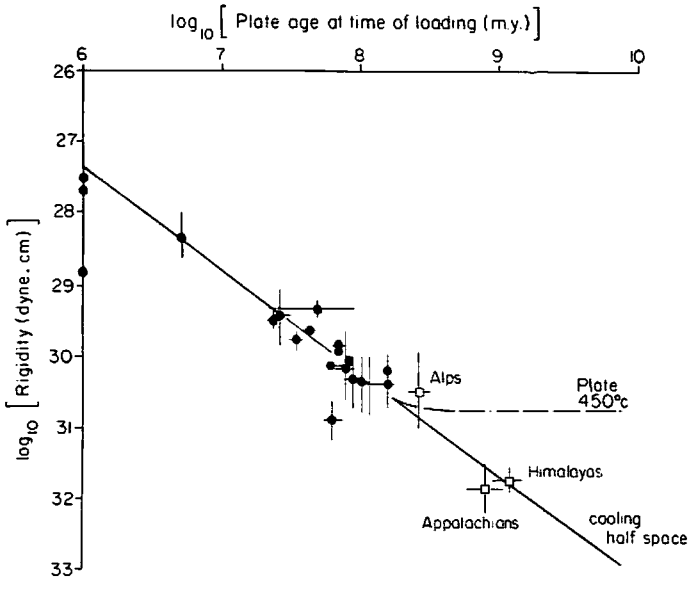


Fig. 19. Plot of $\log_{10}$ (flexural rigidity) against $\log_{10}$ (plate age at time of loading) for oceanic (solid symbols) and continental rigidities determined from this study (open symbols). Note that the continental rigidity estimates appear to have the same trend as defined by the oceanic values. Thus rigidity of the continental lithosphere appears to be dependent on its thermal age at the time of loading. The dashed and solid lines are the equivalent rigidity for the depth of the 450°C isotherm based on the cooling plate model and cooling half-space model, respectively.

tivation of older preexisting faults. For example, in the Alpine foreland the position of the maximum bending stress correlates with the Rhone, Bresse, and Rhine grabens, all of which were reactivated/created during the Alpine orogeny [*Trümpy*, 1973; *Sengör and Burke*, 1978; *Burke*, 1978].

It appears that the flexural response of the continental lithosphere at a mountain range can be partitioned into a primary and secondary deflection. The primary deflection is associated with subsurface loading and so will be independent of surface erosion. However, the secondary deflection associated with the surface topography will with time become eroded and redistributed. During the removal of this surface load we would expect that the plate will rebound. Contrary to the interpretation of *Kahle et al.* [1980], maximum uplift rates appear to correlate with topography rather than crustal structure. Therefore the observed neotectonic movements of the studied mountain ranges may in part be explained by the erosion and subsequent rebound associated with the secondary loads.

## CONCLUSIONS

We made the following conclusions from this study:

1. The pattern of gravity anomalies observed over the mountain ranges studied are generally similar. The characteristic pattern is a positive-negative anomaly "couple." The positive anomalies reach widths of 100–200 km and amplitudes of 50–120 mGal, and the negative anomalies reach widths of 100–400 km and amplitudes of 100–200 mGal.

2. The gravity anomaly patterns can be explained by

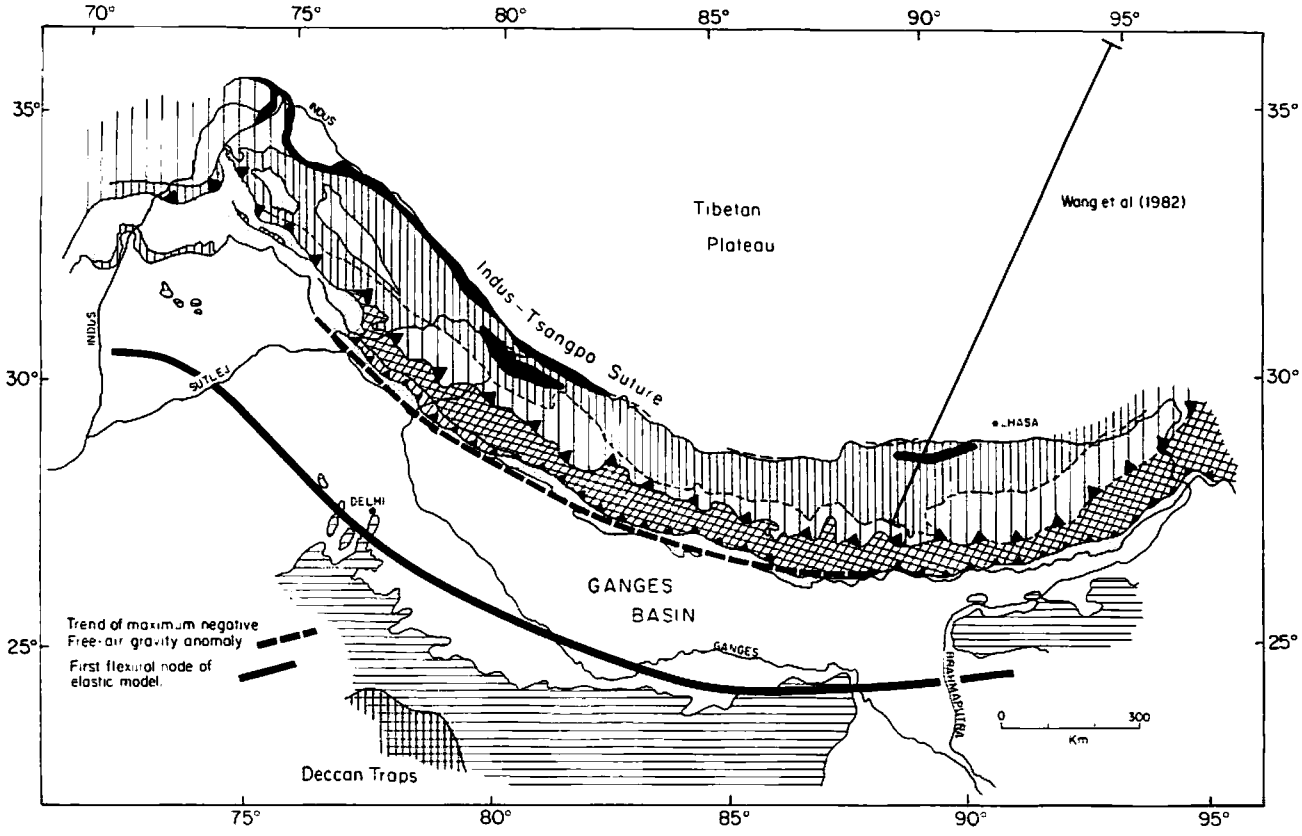


Fig. 20. Summary geological map of northern India showing the position of the major flexural features predicted by the model applicable for the loading scheme of the Himalayas.

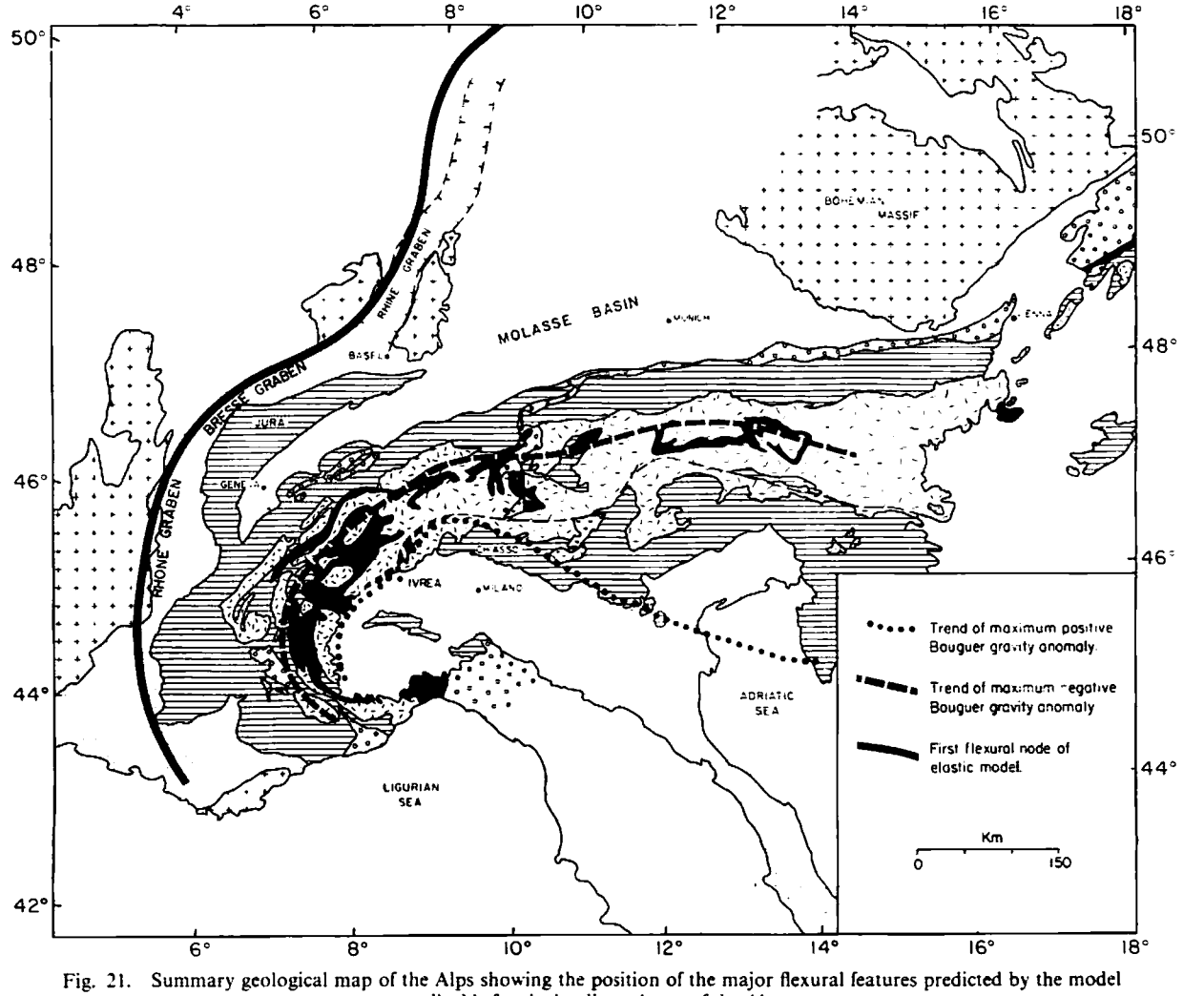


Fig. 21. Summary geological map of the Alps showing the position of the major flexural features predicted by the model applicable for the loading scheme of the Alps.

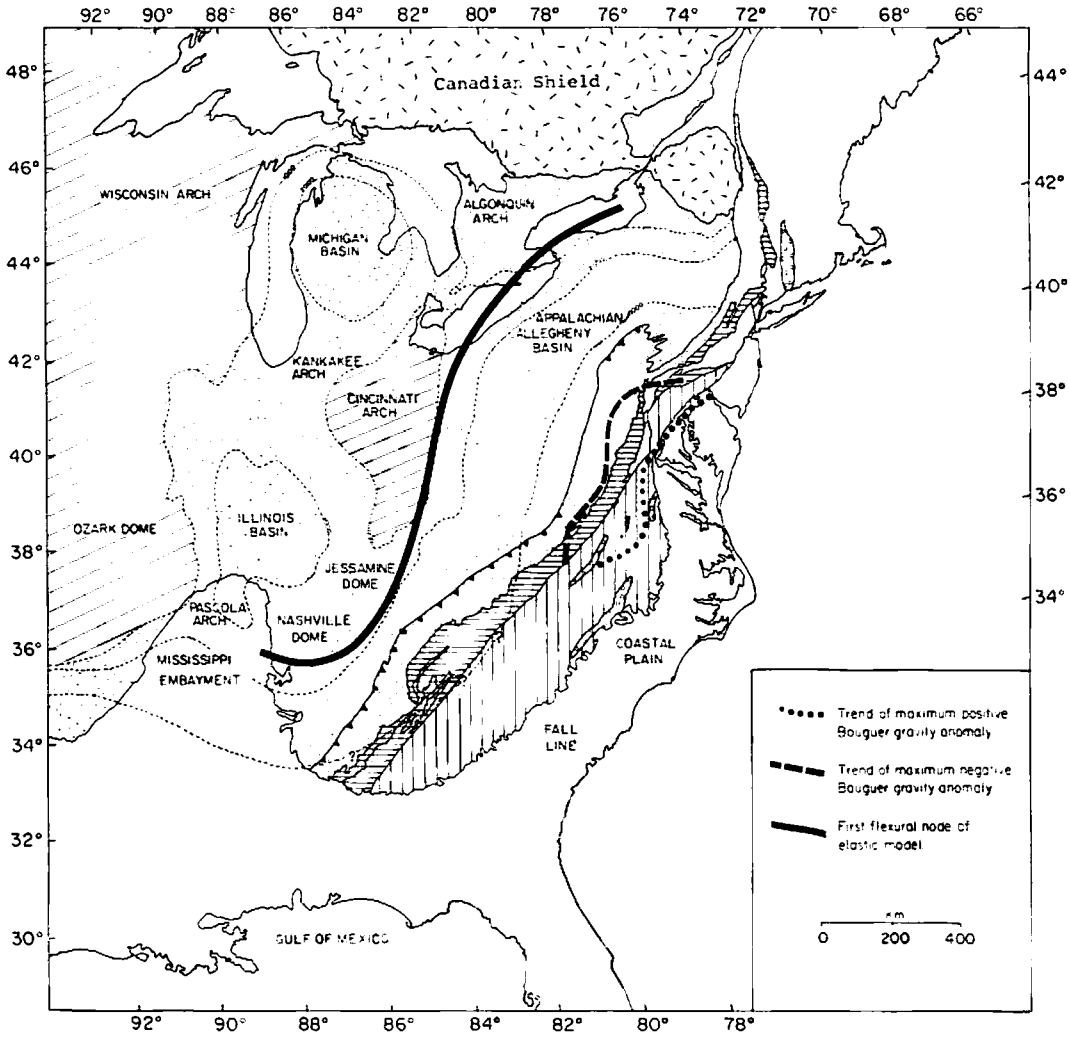


Fig. 22. Summary geological map of the Appalachians showing the position of the major flexural features predicted by the model applicable for the loading scheme of the Appalachians.

simple models of flexure in which the lithosphere at mountain ranges is deformed by surface and subsurface loads. The most likely cause of these loads are the fold/thrust belts (surface loads) and obducted blocks/flakes (subsurface loads) that develop during continental collision, suturing, and convergence.

3. The preservation of thick sedimentary sequences within a molasse basin, even when the associated mountain range has been significantly reduced by erosion, suggests that loads, independent of both surface topography and crustal blocks, must exist. Although the nature and origin of these additional loads are not known, they may be related to either the preorogenic crustal structure of the colliding plates or perhaps to crustal thinning associated with back arc rifting processes during active subduction.

4. The gravity anomaly at a mountain range is the summation of the effect of all the surface and subsurface loads acting on the lithosphere and the associated sediment-filled depressions caused by these loads. By estimating the magnitudes of all the loads acting on the lithosphere, we have estimated the elastic thickness $T_e$ (or the equivalent flexural rigidity) of the continental lithosphere at a mountain range to be in the range 25–50 (Alps) to 80–130 km (Appalachians, Himalaya).

5. The significant role of subsurface loading in explaining the observed gravity anomaly suggests that the location of the greatest depression of crustal layers and/or the M discontinuity may not necessarily correspond to the location of the peak elevation at mountain ranges. This suggestion, based on gravity arguments, is in general agreement with available seismic refraction data, at least in the central Alps.

6. The maximum depression of the M discontinuity at a mountain range corresponds instead to the location of the center of mass of all the loads (surface and subsurface) that act on the lithosphere during mountain building.

7. The subsurface load contributes most, not only to the observed gravity anomaly, but also to the amplitude and wavelength of the flexural basins that form during mountain building. Surface loads also contribute, but their total effect is small compared to subsurface loads. Thus subsurface loads probably control the overall location of the depocentre in postorogenic (molasse-type) basins, while surface loads control local variations in the location of the depocenter. Both loads (surface and subsurface), however, contribute to migration of the outer flexural arch and foreland basement onlap at the edges of postorogenic basins.

8. The gravity anomaly patterns over mountain ranges are consistent with the emplacement of the obducted block/flake as the primary event during mountain building that control the overall shape of the postorogenic basins and the development of fold/thrust belts flanking the core zone. Thus the formation of topography by fold/thrust belts is a secondary event during mountain building.

9. Lithospheric flexure appears to be an important mechanism in controlling the formation and development of arches, swells, and passive rift zones within the continental basement flanking mountain ranges. Because of the high overall flexural rigidity of continental lithosphere, the effects of flexure can extend for $\gtrsim 1000$ km from the loads associated with mountain building.

## APPENDIX A: DATA BANK SYSTEM ADOPTED FOR USE WITH GRAVITY AND TOPOGRAPHY DATA

The data bank system is based on the concept of data bins. The world is basically subdivided into geographical compartments or bins, the boundaries of which form an integer grid of latitude and longitude. With the world's surface binned, any gravity station will naturally belong to a unique bin. Because of the detailed coverage of land and marine gravity data, the bin size chosen was 1° × 1°. The bins are stored on computer disk with a unique file name created from the latitude and longitude of the bin's bottom left-hand corner. Complete details of this system are given by *Karner* [1981].

Each record stored within a bin contains the latitude, longitude, absolute gravity, topography, free air gravity, Bouguer gravity, various processing flags, and, finally, alphanumeric information relating to the data source. The free air gravity anomaly, both marine and continental data, is referred to the International Gravity Standardization Net (1980) reference system which includes a Potsdam correction of −14 mGal. Only measured point gravity and topography information is stored in the data bank.

A computer program was written to project automatically the gravity and topography data onto a great circle joining the coordinates of the profile end points. Figure A1, showing a portion of the data distribution in northern India, demonstrates the projection procedure. The baseline is defined by the great circle joining the coordinates (25.25.075) and (30,080). In addition to the baseline, a data window is also defined, which in this example, is ±50 km either side of the baseline. All data lying between the baseline coordinates and within the window are orthogonally projected onto the baseline, of which a few examples are shown in Figure A1. The bins through which the great circle and its envelope pass are automatically opened and the enclosed data extracted and projected. Output is two files containing the projected topographic and gravimetric data.

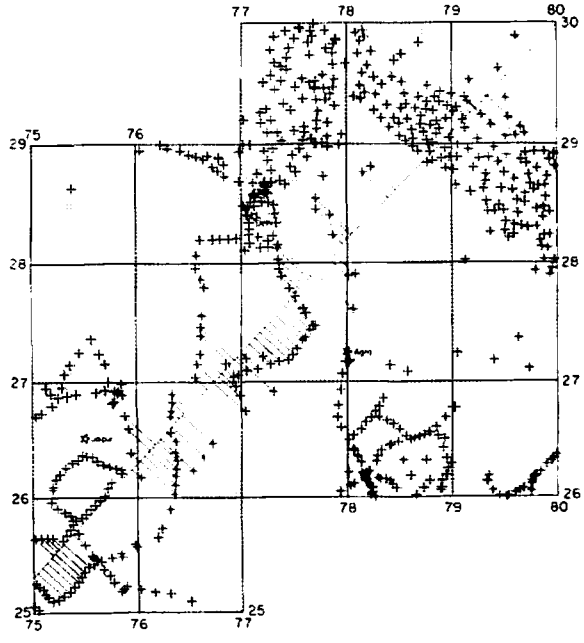


Fig. A1. Plot of the data positions contained within 20 bins from northern India used to construct profile C (Figure 4). A bin is a 1° × 1° geographical square. The line from latitude 25.25°N, longitude 75°E to latitude 30°N, longitude 80°E is the projection line onto which the data contained within a given window width (unshaded area) are orthogonally projected.

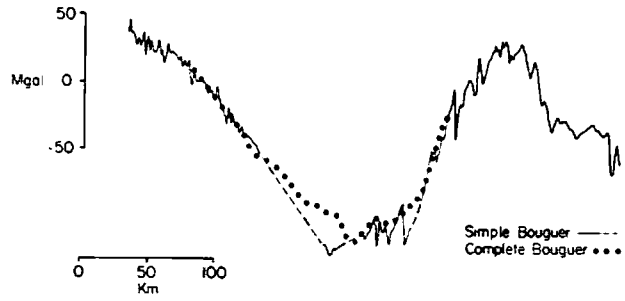


Fig. A2. Comparison between simple and complete Bouguer anomalies along the Swiss geotraverse. The simple Bouguer anomaly was calculated from free air gravity and topography data prepared from the binning system (Appendix B) by using a topographic density of 2.67 g cm$^{-3}$. The complete Bouguer anomaly is from *Kahle et al.* [1976]. The main difference between the two anomalies occurs at wavelengths $\lesssim 40$ km with amplitudes 20–30 mGal. Since this study is concerned with wavelengths $>100$ km and amplitudes 100–200 mGal, the simple Bouguer anomaly is a satisfactory approximation to the complete Bouguer anomaly over mountain ranges for these wavelengths.

Data distribution can cause serious problems especially with large projection windows. For example, the data distribution near the town of Jaipur (Figure A1) is limited to the road network in the area. Since the location of the roads tend to oscillate across the baseline, regional gravity (or topographic) gradients across the window may be aliased into the projected profile. This is probably the source of the high-frequency gravity variations seen in profile C (Figure 4). For this reason, it was advantageous to filter the recalculated Bouguer gravity anomaly with a Gaussian filter. For Figures 4, 5, and 6, the standard deviation is $\sigma = 5$ km; for Figure 15, $\sigma = 40$ km.

In mountain regions it is very common to measure gravity along roads which invariably are in valleys. The projected topographic profiles are necessarily, therefore, only an approximation to the true shape of the mountains. However, we believe that the absence of mountain peaks will not seriously effect our volume estimates used to determine the surface load.

There is a further problem with gravity from mountain regions. Simple Bouguer gravity anomalies from mountains and adjacent regions may be underestimated because of the additional gravity effect of mountain peaks and valleys poorly approximated by the Bouguer slab formula. The terrain correction, as it is called, is essentially a near-field effect and is always positive. The use of simple Bouguer anomalies in this paper is justifiable in terms of the amplitudes and wavelength of the gravity anomalies being interpreted. Figure A2 com-

Fig. A3. (opposite) Data sampling density of the bins used to construct the projected profiles for each of the mountain ranges. The darker the tone of any 1° square, the greater the sampling density.

HIMALAYAS

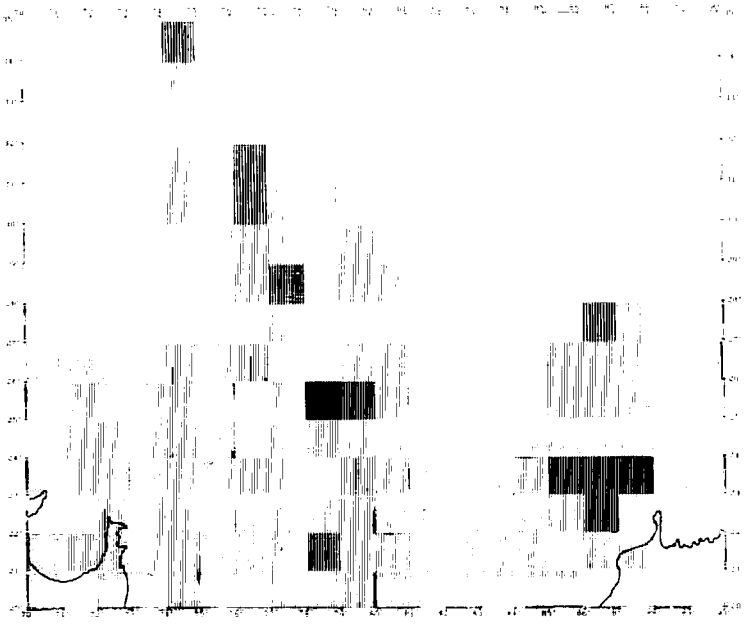

ALPS

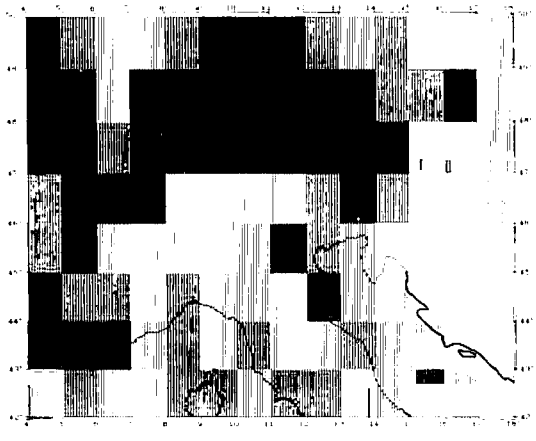

KEY (number of points/bin)

- >1000
- 500-999
- 200-499
- 100-199
- 25-99
- 1-24
- 0

APPALACHIANS

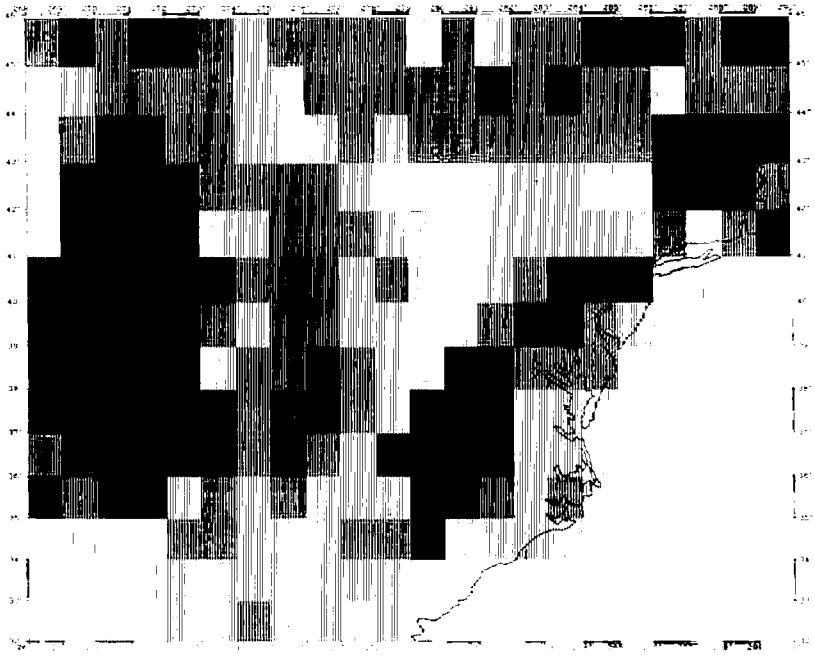

pares both the simple and terrain-corrected (complete) Bouguer gravity anomalies along the Swiss geotraverse (profile K, Figure 3). The simple Bouguer anomaly was recalculated from free air gravity and topography data supplied by DMA using a topographic density of 2.67 g cm$^{-3}$. The complete Bouguer anomaly is from *Kahle et al.* [1976]. The main difference between the two profiles, as expected, is over the mountain range. For this traverse the wavelength of the terrain correction is ~40 km with an amplitude of 20–30 mGal. As the anomaly being interpreted has wavelengths > 100 km and amplitude 100–200 mGal, the terrain correction for this study is not considered crucial.

Figure A3 summarizes the data distribution within the three areas studied. Both the Alps and Appalachians have been well sampled geographically, the studied area containing $10^4$–$10^5$ stations. Because of the close data sampling, we reduced the window, thereby reducing aliasing problems. The Himalayas, however, have a significantly lower data-sampling density relative to the other two mountains and this necessitates a wider sampling window. Nevertheless, the Himalayan study area contains $10^3$–$10^4$ stations.

## Appendix B: Theory for Investigation of Role of Flexure in Development of Mountain Ranges

Since suture zones represent either existing or surface expressions of former major tectonic boundaries between opposing lithospheric plates that were active at some time during the development of mountain ranges, it would seem appropriate to assume that each plate acts as a cantilever. In this respect, the long-term deformation of the opposing plates can be approximated by the deflection of a broken elastic plate overlying a weak fluid substratum. A similar mechanical model has been used to model deep-sea trench outer rise systems [*Gunn*, 1947; *Walcott*, 1970; *Hanks*, 1971; *Watts and Talwani*, 1974; *Bodine and Watts*, 1979].

The flexure of a broken plate can be considered a special case of the general loading of a continuous plate. The difference is that the bending moment and shearing force created by the distributed load throughout the continuous plate are counterbalanced by opposing forces at the position of the break (suture). An opposing moment and shear force create the required so-called "end-conditioning" forces at the position of the presumed break [*Hetényi*, 1946]. Thus the equations describing the flexure of a broken elastic plate can be simply derived from the deflection equation for the loading of a continuous plate.

It is advantageous to optimize the calculation of the deflection of a thin elastic plate by considering only the applied load spectrum, thereby negating the need to consider the load as a collection of squares and/or triangles (cf. space domain equations of *Hetényi* [1946]).

The deflection of a continuous elastic plate caused by a distributed load [*Banks et al.*, 1977] can be expressed in the frequency domain as

$$Y_c(k) = \frac{\Delta\rho_1}{\Delta\rho_4}\,\Phi_c H(k) \tag{B1}$$

$$\Phi_c = \left[1 + \frac{Dk^4}{\Delta\rho_4 g}\right]^{-1}$$

where $Y_c(k)$ is the plate response in the wave domain ($y_c(x)$ is the deflection in the space domain) to the applied load (surface or subsurface) spectrum $H(k)$, $\Delta\rho_1$ is the density contrast of the load, $\Delta\rho_4$ is the density contrast between the material underlying the plate and the material infilling the deflection, $k$ is the wavenumber which is related to the load wavelength $\lambda$ by $k = 2\pi/\lambda$, and $g$ is average gravity. $D$, the flexural rigidity of the elastic plate, determines the deflection wavelength and amplitude and is defined as

$$D = ET_e^3/12(1 - \nu^2) \tag{B2}$$

where $E$ is Young's modulus, $T_e$ the elastic thickness of the plate, and $\nu$ is Poisson's ratio. The bending moment and shearing force are proportional to the curvature of the deflection and the derivative of the curvature, respectively, viz.,

$$M(x) = -D\frac{d^2}{dx^2}\,y_c(x) \tag{B3}$$

$$Q(x) = -D\frac{d^3}{dx^3}\,y_c(x) \tag{B4}$$

Equations (B1)–(B4) relate only to a continuous plate. It is not possible, however, to use a simple wave domain product (as in equation (B2)) to determine the deflection spectrum for a load on a broken plate. This is because a simple wave domain product (a space domain convolution) is independent of the origin. For a broken plate it is necessary to define an origin; hence making the equations $x$ shift variant. Assuming the origin at $x = x_0$, the end-conditioning forces $P_0$ and the bending moment $M_0$ can be ogtained by [*Hetényi*, 1946]

$$P_0 = 4[\lambda M(x_0) + Q(x_0)] \tag{B5}$$

$$M_0 = -2\left[2M(x_0) - \frac{Q(x_0)}{\lambda}\right] \tag{B6}$$

where

$$\lambda^{-4} = 4D/\Delta\rho_4 g \tag{B7}$$

The continuous plate deflection spectrum implied by these end-conditioning forces is

$$Y_c(k) = \frac{4\lambda^4}{\Delta\rho_4 g(4\lambda^4 + k^4)}\,[P_0 + M_0 ki] \tag{B8}$$

The total deflection spectrum of the continuous plate considering the applied surface load and end-conditioning forces becomes

$$Y_b(k) = Y_e(k) + Y_c(k)$$

$$= \Phi_e\left[\frac{P_0 + \Delta\rho_1 g H_r(k)}{\Delta\rho_4 g} + \frac{M_0 k_i + \Delta\rho_1 g H_i(k)}{\Delta\rho_4 g}\right] \tag{B9}$$

where $H_r(k)$ is the real part of $H(k)$ and $H_i(k)$ is the imaginary part of $H(k)$. With these forces and moments acting on the plate, the deflection of the continuous plate will correspond to that of a broken plate with an origin at $x = x_0$.

To calculate the free air gravity effect of the load and plate deflection, we use the first four terms of the Fourier domain relationship between load and deflection defined by *Parker* [1973]. The general equation for the gravity effect of a two-layer crustal model is obtained by summing the effects of the load and the individual crustal layers, viz.,

$$G_{\text{load}}(k) = 2\pi\gamma \sum_{n=1}^{4} \frac{k^{n-1}}{n!}\,(\Delta\rho_1\, H_1{}^n(k) + \Delta\rho_3 H_2{}^n(k)e^{-kd_2}) \tag{B10}$$

$$G_{\text{basement}}(k) = -2\pi\gamma\,\Delta\rho_2 e^{-kd_3} \sum_{n=1}^{4} \frac{k^{n-1}}{n!}\,Y_b{}^n(k) \tag{B11}$$

where $\Delta\rho_1$ is the density of the surface load, $\Delta\rho_2$ is the density contrast between the sediment infill and the basement, $\Delta\rho_3$ is the density contrast between the basement and mantle, $H_1(k)$ is the Fourier transform of the surface load, $H_2(k)$ is the Fourier transform of the subsurface load, $d_2$ is the median depth of the subsurface load, and $d_3$ is the median depth of the deflected basement. In addition,

$$G_{\text{Moho}}(k) = -2\pi\gamma\,\Delta\rho_3 \exp\left[-k(d_1 + d_3)\right] \sum_{n=1}^{4} Y_b^n(k) \qquad \text{(B12)}$$

where $d_1$ is the median depth to the M discontinuity. Therefore the total gravity effect is given by

$$G_{\text{total}}(k) = G_{\text{load}}(k) + G_{\text{basement}}(k) + G_{\text{Moho}}(k) \qquad \text{(B13)}$$

*Acknowledgments.* We thank K. Jacob, M. McNutt, C. Burchfiel, I. Dalziel, J. Cochran, and N. Ribe for critically reviewing the paper and W. Haxby, J. Weissel, and J. Thorne for the many fruitful discussions concerning the concepts and techniques presented in this paper. The Defense Mapping Agency (Missouri) kindly provided much of the topographic and gravimetric data used in this study. This work was supported by National Science Foundation contracts OCE 79-18917 and EAR 81-09473 and an Australian Public Service Postgraduate Scholarship (GDK). Lamont-Doherty Geological Observatory contribution 3540.

## REFERENCES

Airy, G. B., On the computation of the effect of the attraction of mountain masses as disturbing the apparent astronomical latitude of stations of geodetic surveys, *Philos. Trans. R. Soc. London, 145*, 101–104, 1855.

Bally, A. W., P. L. Gordy, and G. A. Stewart, Structure, seismic data and orogenic evolution of the southern Canadian Rocky mountains, *Bull Can. Pet. Geol., 14*, 337–381, 1966.

Banks, R. J., R. L. Parker, and S. P. Huestis, Isostatic compensation on a continental scale: Local versus regional mechanisms, *Geophys. J. R. Astron. Soc., 51*, 431–452, 1977.

Barazangi, M., and J. Ni, Velocities and propagation characteristics of $P_n$ and $S_n$ beneath the Himalayan arc and Tibetan plateau: Possible evidence for underthrusting of Indian continental lithosphere beneath Tibet, *Geology, 10*, 179–185, 1982.

Beach, A., Thrust structures in the eastern Dauphinois Zone (French Alps), north of the Pelvous Massif, *J. Struct. Geol., 3*, 299–308, 1981.

Beaumont, C., Foreland basins, *Geophys. J. R. Astron. Soc., 65*, 291–329, 1981.

Bhattacharya, S. N., Seismic surface-wave dispersion and crust-mantle structure of the Indian Peninsula, *Indian J. Meteorol. Geophys., 22*, 179–186, 1971.

Bird, P., and M. N. Toksoz, Strong attenuation of Rayleigh waves in Tibet, *Nature, 266*, 161–163, 1977.

Bodine, J. H., and A. B. Watts, On lithospheric flexure seaward of the Bonin and Mariana trenches, *Earth Planet. Sci. Lett., 43*, 132–148, 1979.

Bowie, W., *Isostasy*, 275 pp., Dutton, New York, 1927.

Brooks, M., Positive Bouguer anomalies in some orogenic belts, *Geol. Mag., 111*, 399–400, 1970*a*.

Brooks, M., A gravity survey of coastal areas of West Finnmark, Northern Norway, *Q. J. Geol. Soc. London, 125*, 171–192, 1970*b*.

Brown, L. D., J. E. Oliver, S. Kaufman, J. A. Brewer, F. A. Cook, F. S. Schilt, D. S. Albaugh, and G. H. Long, Deep crustal structure: Implications for continental evolution, in *Evolution of the Earth, Geodyn. Ser.*, vol. 5, edited by R. J. O'Connell and W. S. Fyfe, pp. 38–52, AGU, Washington, D. C., 1981.

Burke, K., Evolution of continental rift systems in the light of plate tectonics, in *Tectonics and Geophysics of Continental Rifts*, edited by I. A. Ramberg and E. R. Neumann, NATO Advanced Study Institute, 1978.

Caldwell, J. G., and D. L. Turcotte, Dependence of the thickness of the elastic oceanic lithosphere on age, *J. Geophys. Res., 84*, 7572–7576, 1979.

Cassinis, R., R. Franciosi, and S. Scarascia, The structure of the earth's crust in Italy—A preliminary typology based on seismic data, *Boll. Geofis. Teor. Appl., 21*, 105–126, 1979.

Cermak, V., Heatflow map of Europe, in *Terrestrial Heatflow in Europe*, edited by V. Cermak and L. Rybach, pp. 3–40, Springer-Verlag, New York, 1979.

Chamberlin, R. T., Isostasy from the geological point of view, *J. Geol., 39*, 1–23, 1931.

Chandra, U., Seismicity, earthquake mechanisms, and tectonics along the Himalayan mountain range and vicinity, *Tectonphysics, 16*, 109–131, 1978.

Choudhury, M., P. Giese, and G. de Visintine, Crustal structure of the Alps—Some general features from explosion seismology, *Boll. Geofis. Teor. Appl., 13*, 211–240, 1971.

Chun, K., and T. Yoshii, Crustal structure of the Tibet Plateau: A surface wave study by a moving window analysis, *Bull. Seismol. Soc. Am., 67*, 735–750, 1977.

Clar, E., Review of the structure of the eastern Alps, in *Gravity and Tectonics*, edited by K. A. deJong and R. Scholten, pp. 253–270, John Wiley, New York, 1973.

Cook, F. A., D. S. Albough, L. D. Brown, S. Kaufman, J. E. Oliver, and R. D. Hatcher, Thin-skinned tectonics in the crystalline southern Appalachians: COCORP seismic-reflection profiling of the Blue Ridge and Piedmont, *Geology, 7*, 563–567, 1979.

Daignieres, M., J. Gallart, E. Banda, and A. Hirn, Implications of the seismic structure for the orogenic evolution of the Pyrenean range, *Earth Planet. Sci. Lett., 57*, 88–100, 1982.

Dewey, J. F., Ophiolite obduction, *Tectonophysics, 31*, 93–120, 1976.

Dewey, J. F., Suture zone complexities: A review, *Tectonophysics, 40*, 53–67, 1977.

Dietrich, V. J., Evolution of the Eastern Alps: A plate tectonics working hypothesis, *Geology, 3*, 147–152, 1975.

Dietrich, V., Ophiolite belts of the central Mediterranean, *Geol. Soc. Am. Map Chart Ser., MC33*, sheet 2, 1979.

Diment, W. H., Gravity anomalies in northwestern New England, in *Studies of Appalachian Geology: Northern and Maritime*, edited by E. Zen et al., pp. 399–413, John Wiley, New York, 1968.

Dorman, L. M., and B. T. R. Lewis, Experimental isostasy, 1, Theory of the determination of the earth's isostatic response to a concentrated load, *J. Geophys. Res., 75*, 3357–3365, 1970.

Fountain, D. M., and M. H. Salisbury, Exposed cross-sections through the continental crust: Implications for crustal structure, petrology and evolution, *Earth Planet. Sci. Lett., 56*, 263–277, 1981.

Gansser, A., *The Geology of the Himalayas*, 289 pp., Interscience, New York, 1964.

Gibb, R. A., and M. D. Thomas, Gravity signature of fossil plate boundaries in the Canadian Shield, *Nature, 262*, 199–200, 1976.

Giese, P., and C. Prodehl, Main features of crustal structure in the Alps, in *Explosion Seismology in Central Europe*, edited by P. Giese, C. Prodehl, and A. Stein, pp. 347–375, Springer-Verlag, New York, 1976.

Giese, P., K. J. Ruetter, V. Jacobshagen, and R. Nicolich, Explosion seismic crustal studies in the Alpine-Mediterranean region and their implications to tectonic processes, in *Alpine-Mediterranean Geodynamics, Geodyn. Ser.*, vol. 7, edited by H. Berkhemer, AGU, Washington, D. C., 1982.

Gunn, R., Quantitative aspects of juxtaposed ocean deeps, mountain chains and volcanic ranges, *Geophysics, 12*, 238–255, 1947.

Gupta, H. K., D. C. Nyman, and M. Landisman, Shield like upper mantle velocity structure below the Indogangetic plains: Inferences drawn from long period surface wave dispersion studies, *Earth Planet. Sci. Lett., 34*, 51–55, 1977.

Gupta, H. K., V. D. Rao, and J. Singh, Continental collision tectonics: Evidence from the Himalaya and the neighboring regions, *Tectonophysics, 81*, 213–238, 1982.

Hanks, T. C., The Kuril Trench–Hokkaido rise system: Large shallow earthquakes and simple models of deformation, *Geophys. J. R. Astron. Soc., 23*, 173–189, 1971.

Harris, L. D., and K. C. Bayer, Sequential development of the Appalachian orogen above a master decollement—A hypothesis, *Geology, 7*, 568–572, 1979.

Hatcher, R. D., Thrusts and nappes in the North American Appalachian orogen, in *Thrust and Nappe Tectonics*, edited by K. R. McClay and N. J. Price, pp. 491–499, Geological Society, London, 1981.

Hatcher, R. D., and A. L. Odom, Timing of thrusting in the southern Appalachians, USA: Model for orogeny? *J. Geol. Soc. London, 137*, 321–327, 1980.

Hayford, J. F., and W. Bowie, The effect of topography and isostatic

compensation upon the intensity of gravity, *Spec. Publ., 10*, U.S. Coast and Geod. Serv., 1912.

Heiskanen, W. A., Untersuchungen über Schwerkraft und Isostasie, *Publ. Finn. Geod. Inst., 4*, 1–96, 1924.

Hetényi, M., *Beams on Elastic Foundation*, 255 pp., University of Michigan Press, Ann Arbor, 1946.

Hsü, J. K., Thin-skinned plate tectonics during neo-Alpine orogenesis, *Am. J. Sci., 279*, 359–366, 1979.

Iverson, W. P., and S. B. Smithson, Master decollement root zone beneath the southern Appalachians and crustal balance, *Geology, 10*, 241–245, 1982.

James, D. E., T. J. Smith, and J. S. Steinhart, Crustal structure of the middle Atlantic states, *J. Geophys. Res., 73*, 1983–2008, 1968.

Johnson, D. W., *Stream Sculpture on the Atlantic Slope: A Study of the Evolution of Appalachian rivers*, Columbia University Press, New York, 1931.

Jordan, T. E., Thrust loads and foreland basin evolution, Cretaceous, western United States, *Am. Assoc. Pet. Geol. Bull., 65*, 2506–2520, 1981.

Kahle, H. G., E. Klingele, S. Mueller, and R. Egloff, The variation of crustal thickness across the Swiss Alps based on gravity and explosion seismic data, *Pure Appl. Geophys., 114*, 479–494, 1976.

Kahle, H. G., S. Mueller, E. Klingele, R. Egloff, and E. Kissling, Recent dynamics, crustal structure, and gravity in the Alps, in *Earth Rheology, Isostasy and Eustasy*, edited by N. A. Mörner, pp. 377–388, John Wiley, 1980.

Kailasam, L. N., Plateau uplift in Peninsular India, *Tectonophysics, 61*, 243–269, 1979.

Kaminski, W., and H. Menzel, Zur Deutung der Schwere anomalie des Ivrea-Körpers, *Schweiz. Mineral. Petrogr. Mitt., 48*, 255–260, 1968.

Kanasewich, E. R., Deep crustal structure under the interior plains and Rocky Mountains, *Can. J. Earth Sci., 3*, 937–945, 1966.

Karner, G. D., Global data bank system, *Tech. Rep. 1, CU-1-81*, 27 pp., Lamont-Doherty Geol. Observ. of Columbia Univ., Palisades, N. Y., 1981.

Karner, G. D., and A. B. Watts, On isostasy at Atlantic-type continental margins, *J. Geophys. Res., 87*, 2923–2948, 1982.

Kent, D. V., and N. D. Opdyke, Paleomagnetism of the Devonian Catskill red beds: Evidence for motion of the coastal New England–Canadian Maritime region relative to cratonic North America, *J. Geophys. Res., 83*, 4441–4450, 1978.

Kent, D. V., and N. D. Opdyke, The early Carboniferous palaeomagnetic field of North America and its bearing on tectonics of the northern Appalachians, *Earth Planet. Sci. Lett., 44*, 365–372, 1979.

King, P. B., Tectonic map of North America, *Map G67154*, U.S. Geol. Surv., Reston, Va., 1976.

Klootwijk, C. T., A review of palaeomagnetic data from the Indian fragment of Gondwanaland, in *Geodynamics of Pakistan*, edited by A. Farah and K. A. de Jong, pp. 41–80, Geological Survey of Pakistan, Islamabad, 1979.

Klootwijk, C. T., Greater India's northern extent and its underthrust of the Tibetan Plateau: Palaeomagnetic constraints and implications, in *Zagros, Hindu Kush, Himalaya—Geodynamic Evolution, Geodyn. Ser.*, vol. 3, edited by H. K. Gupta and F. M. Delany, pp. 313–323, AGU, Washington, D. C., 1981.

Laubsher, H., Jura Mountains, in *Gravity and Tectonics*, edited by K. A. De Jong and R. Scholten, pp. 217–227, John Wiley, New York, 1973.

Laubscher, The 3D propagation of decollement of the Jura, in *Thrust and Nappe Tectonics*, edited by K. R. McClay and N. J. Price, pp. 311–318, Geological Society, London, 1981.

LeFort, P., Himalayas: The collided range. Present knowledge of the continental arc, *Am. J. Sci., 275A*, 1–44, 1975.

Lemoine, M., The Alps, their molassic foredeep and the Jura, in *Geological Atlas of Alpine Europe and Adjoining Alpine Areas*, edited by M. Lemoine, pp. 313–322, Elsevier, New York, 1978.

Lewis, B. T. R., and L. M. Dorman, Experimental isostasy, 2, Isostatic model for the U.S.A. derived from gravity and topography data, *J. Geophys. Res., 75*, 3367–3386, 1970.

McNutt, M. K., Implications of regional gravity for state of stress in the earth's crust and upper mantle, *J. Geophys. Res., 85*, 6377–6396, 1980.

McNutt, M. K., and R. L. Parker, Isostasy in Australia and the evolution of the compensating mechanism, *Science, 199*, 773–775, 1978.

Menard, H. W., and M. K. McNutt, Evidence for and consequences of thermal rejuvination, *J. Geophys. Res., 87*, 8570–8580, 1982.

Miyashiro, A., K. Aki, and A. M. Celâl Sengör, *Orogeny*, 242 pp., John Wiley, New York, 1982.

Molnar, P., and P. Tapponnier, Cenozoic tectonics of Asia: Effects of a continental collision, *Science, 189*, 419–426, 1975.

Mueller, S., A new model of the continental crust, in *The Earth's Crust, Geophys. Monogr. Ser.*, vol. 20, edited by J. G. Heacock, pp. 289–317, Washington, D. C., 1977.

Mueller, S., and M. Talwani, A crustal section across the Eastern Alps based on gravity and seismic refraction data, Pageoph, 85, 226–239, 1971.

Mueller, S., J. Ansorge, R. Egloff, and E. Kissling, A crustal cross-section along the Swiss Geotraverse from the Rhinegraben to the Po Plain, *Eclogae Geol. Helv., 73*, 463–483, 1980.

Müller, W. H., and U. Briegel, Mechanical aspects of the Jura overthrust, *Eclogae Geol. Helv., 73*, 239–250, 1980.

Oxburgh, E. R., Flake tectonics and continental collision, *Nature, 239*, 202–204, 1972.

Pakiser, L. C., and J. S. Steinhart, Explosion seismology in the western hemisphere, in *Research in Geophysics*, vol. 2, *Solid Earth and Interface Phenomena*, edited by H. Odishaw, MIT Press, Cambridge, Mass., 1964.

Parker, R. L., The rapid calculation of potential anomalies, *Geophys. J. R. Astron. Soc., 31*, 447–455, 1973.

Powell, C. M., A speculative tectonic history of Pakistan and surroundings: Some constraints from the Indian Ocean, in *Geodynamics of Pakistan*, edited by A. Farah and K. A. DeJong, pp. 5–24, Geological Survey of Pakistan, Islamabad, 1979.

Powell, C. M., and P. J. Conaghan, Plate tectonics and the Himalayas, *Earth Planet. Sci. Lett., 20*, 1–12, 1973.

Pratt, J. H., On the attraction of the Himalayan Mountains, and of the elevated regions beyond them, upon the plumb line in India, *Philos. Trans. R. Soc., 145*, 53–100, 1855.

Price, R. A., Large-scale gravitational flow of supracrustal rocks, southern Canadian Rockies, in *Gravity and Tectonics*, edited by K. A. deJong and R. Scholten, pp. 491–502, John Wiley, New York, 1973.

Prodehl, C., The structure of the crust-mantle boundary beneath North America and Europe as derived from explosion seismology, in *The Earth's Crust, Geophys. Monogr. Ser.*, vol. 20, edited by J. G. Heacock, pp. 349–369, AGU, Washington, D. C., 1977.

Putnam, G. R., Results of transcontinental series of gravity measurements, *Bull. Washington Philos. Soc., 13*, 61, 1895.

Rodgers, J., *The Tectonics of the Appalachians*, 271 pp., Interscience, New York, 1970.

Rudman, A. J., C. H. Summerson, and W. J. Hinze, Geology of basement in midwestern United States, *Am. Assoc. Pet. Geol. Bull., 49*, 894–904, 1965.

Rybach, L., S. Mueller, A. G. Milnes, J. Ansorge, D. Bernoulli, and M. Frey, The Swiss Geotraverse Basel–Chiasso—A review, *Eclogae Geol. Helv., 73*, 437–462, 1980.

Sandwell, D. T., and G. Schubert, Geoid height-age relation from SEASAT altimeter profiles across the Mendocino fracture zone, *J. Geophys. Res., 87*, 3949–3958, 1982.

Sastri, V. V., L. L. Bhandari, A. T. R. Ragu, and A. K. Datta, Tectonic framework and subsurface stratigraphy of the Ganga Basin, *J. Geol. Soc. India, 12*, 222–233, 1971.

Schenk, V., Synchronous uplift of the lower crust of the Ivrea zone and of southern Calabria and its possible consequences for the Hercynian orogeny in southern Europe, *Earth Planet. Sci. Lett., 56*, 305–320, 1981.

Seeber, L., and J. G. Armbruster, The 1886 Charleston, South Carolina, earthquake and the Appalachian detachment, *J. Geophys. Res., 86*, 7874–7894, 1981.

Seeber, L., J. G. Armbruster, and R. Quittmeyer, Seismicity and continental subduction in the Himalayan arc, in *Zagros, Hindu Kush, Himalaya Geodynamic Evolution, Geodyn. Ser.*, vol. 3, edited by H. K. Gupta and F. M. Delany, pp. 215–242, AGU, Washington, D. C., 1981.

Sengör, A. M. C., and K. Burke, Relative timing of rifting and volcanism on earth and its tectonic implications, *Geophys. Res. Lett., 5*, 419–421, 1978.

Shackleton, R. M., Structure of southern Tibet: Report on a traverse from Lhasa to Khatmandu organized by Academia Sinica, *J. Struct. Geol., 3*, 97–105, 1981.

Soper, N. J., and A. J. Barber, A model for the deep structure of the Moine thrust zone, *J. Geol. Soc. London, 139*, 127–138, 1982.

Stephenson, R., and C. Beaumont, Small-scale convection in the upper mantle and the isostatic response of the Canadian Shield, in

*Mechanisms of Continental Drift and Plate Tectonics*, edited by D. Davies and K. Runcorn, pp. 111–122, Academic, New York, 1980.

Tanner, J. G., A geophysical interpretation of structural boundaries in the eastern Canadian shield, Ph.D. thesis, Univ. of Durham, Durham, United Kingdom, 1969.

Tanner, J. G., and R. J. Uffen, Gravity anomalies in the Gaspé Peninsula, Quebec, *Publ. Dom. Observ. Ottawa, 21*, 217–260, 1960.

Teng, J., et al., Characteristic of the geophysical fields and plate tectonics of the Qinghzi-Xinzang Plateau and its neighboring regions, *Acta Geophys. Sinica, 23*, 254, 1980.

Trümpy, R., The timing of orogenic events in the central Alps, in *Gravity and Tectonics*, edited by K. A. deJong and R. Scholten, pp. 229–252, John Wiley, New York, 1973.

Turcotte, D. L., and G. Schubert, *Geodynamics, Applications of Continuum Physics to Geological Problems*, 450 pp., John Wiley, New York, 1982.

Van der Voo, R., and J. E. T. Channell, Palaeomagnetism in orogenic belts, *Rev. Geophys. Space Phys., 18*, 455–481, 1980.

Walcott, R. I., Flexural rigidity, thickness and viscosity of the lithosphere, *J. Geophys. Res., 75*, 3941–3954, 1970.

Wang, C. Y., Y. Shi, and W. H. Zhou, On the tectonics of the Himalaya and the Tibet plateau, *J. Geophys. Res., 87*, 2949–2957, 1982.

Warsi, W. E. K., and P. Molnar, Gravity anomalies and plate tectonics in the Himalaya, in *Colloquium International CNRS, Ecologie et Geologie de l'Himalaya*, vol. 2, pp. 463–478, Centre National de la Recherche Scientifique, Verrières-le-Buisson, France, 1977.

Watts, A. B., An analysis of isostasy in the world's oceans, 1, Hawaiian-Emperor seamount chain, *J. Geophys. Res., 83*, 5989–6004, 1978.

Watts, A. B., The U.S. Atlantic continental margin: Subsidence history, crustal structure and thermal evolution, in *Geology of Passive Continental Margins: History, Structure, and Sedimentologic Record, Educ. Course Note Ser.*, vol. 19, American Association of Petroleum Geologists, Tulsa, Okla., 1981.

Watts, A. B., and M. S. Steckler, Subsidence and eustasy at the continental margin of eastern North America, in *Deep Drilling Results in the Atlantic Ocean: Continental Margins and Paleo environment, Maurice Ewing Ser.*, vol. 3, edited by M. Talwani, W. Hay, and W. B. Ryan, pp. 218–234, AGU, Washington, D. C., 1979.

Watts, A. B., and M. Talwani, Gravity anomalies seaward of deep-sea trenches and their tectonic implications, *Geophys. J. R. Astron. Soc., 36*, 57–90, 1974.

Watts, A. B., J. H. Bodine, and M. S. Steckler, Observations of flexure and the state of stress in the oceanic lithosphere, *J. Geophys. Res., 85*, 6369–6376, 1980.

Watts, A. B., G. D. Karner, and M. S. Steckler, Lithospheric flexure and the evolution of sedimentary basins, *Philos. Trans. R. Soc. London, Ser. A, 305*, 249–281, 1982.

Wilson, C. W., and R. G. Stearns, Quantitative analysis of Ordovician and younger structural development of Nashville Dome, Tennessee, *Bull. Am. Assoc. Pet. Geol., 47*, 823–832, 1963.

G. D. Karner and A. B. Watts, Lamont-Doherty Geological Observatory, Palisades, NY 10964.

(Received December 27, 1982;
revised May 7, 1983;
accepted June 30, 1983.)